DESIGN OF PLANAR AND COMPACT UWB MICROSTRIP ANTENNA WITH BAND REJECTION FEATURES

A Thesis Submitted in Partial Fulfilment of the Requirement for the Award of the Degree of

MASTER OF ENGINEERING

in

ELECTRONICS AND COMMUNICATION ENGINEERING

Submitted by

PARAMITA MAITI

801661016

Under Supervision of

Dr. Jaswinder Kaur

Assistant Professor, ECED

ELECTRONICS AND COMMUNICATION ENGINEERING DEPARTMENT

THAPAR INSTITUTE OF ENGINEERING & TECHNOLOGY
(A DEEMED TO BE UNIVERSITY), PATIALA, PUNJAB
JULY, 2018

DECLARATION

I, Paramita Maiti hereby declare that the work presented in this thesis entitled, "Design of Planar and Compact UWB Microstrip antenna with band rejection features" in fulfilment of the requirement for the award of degree of Master of Engineering (ME Electronics and Communication) submitted at Electronics and Engineering Department, Thapar Institute of Engineering & Technology (Deemed to be University), Patiala is an authentic record of work carried out under supervision of Dr. Jaswinder Kaur, Assistant Professor, Electronics and Communication Engineering Department, Thapar Institute of Engineering & Technology (Deemed to be University), Patiala. The matter presented in this has not been submitted either in part or full to any other university or institute for the award of any other degree.

Paramita Maiti.

Date: 13.7.2018

(Paramita Maiti)
(801661016)

Jaswinder Kaur 13/07/18.

Dr. Jaswinder Kaur
Assistant Professor
Electronics and Communication Engineering Department
Thapar Institute of Engineering & Technology
(A Deemed to be University)
Patiala, Punjab

Date:

ACKNOWLEDGEMENT

This thesis report is completed with prayers and love of my family and friends. However, I would like to specially acknowledge and extend deep sense of exaltation and gratitude to my supervisor **Jaswinder Kaur, Assistant Professor** for her sincere and invaluable guidance, overwhelming inspiration and encouragement in nurturing my thesis work. It has been a blessing for me to spend many auspicious under the guidance of the perfectionists.

I am also grateful to **Dr. Alpana Agarwal, Associate Professor and Head** and all the faculty members of the Electronics and Communication Engineering Department for their help and encouragement. I also place on record, my sense of gratitude to one and all who, directly or indirectly, have lent their helping hand in this venture.

Lastly, I would also like to thank my children, husband and parents for their years of unyielding love and encouragement.

Paramita Maiti

Roll No.: 801661016

ABSTRACT

In today's world wireless is quickest flourishing zone in the communication region. Wireless Local Area Network (WLAN) and Worldwide Interoperability for Microwave Access (WiMAX) technologies are the maximum swiftly rising areas in the contemporary wireless communication. This truly possesses users the flexibility to travel around within a wide region but at the same time connected with the network. In the present environment, technology needs antennas that can function on various wireless bands and must possess versatile features as low cost, light weight, low profile antennas which are able to support high execution over a vast spectrum of frequencies. In the present atmosphere, technology requires ultra-wideband antennas that can function at a broader range of frequency and at the same time with a minimum level of power. But as there are huge number of narrow wireless frequency bands exists in the same ultra-wide band, these creates interference. Hence, there is a necessity of competent and a superior execution antenna which functions at UWB but at the same time discards the interfering bands. With an aim of having transmission in frequency bands except WLAN, WiMAX etc., it is significant to discard these interfering bands at the UWB range used in a broader range globally. In this thesis report, various techniques for discarding the interfering bands in the UWB antenna are conferred. The aim is partially fulfilled by implanting various slots on patch and ground of UWB antenna. In the first design, two arc shaped slots are etched from the patch to reject WiMAX and ARN band; two symmetrical slits are etched from the CPW ground to reject WLAN; rectangular SRRs are etched from the feed line to reject ITU-8 and two symmetrical circular SRRs are etched from the lower part of the patch to reject amature radio band. Simulations are done on CST Studio 2014. In the second design, a single composite parasitic element is used to reject three bands e.g. fixed satellite mobile except aeronautical mobile, aeronautical radio navigation, earth exploration satellite, maritime satellite. The band notched UWB antennas are then fabricated and tested using FR-4 substrate of thickness 1.6 mm. The antenna is tested using Agilent VNA model no. E5071C. The measured and simulated results are compared. The measured and simulated results obtained are similar to each other with a slight variation.

Keywords: UWB antenna, band notch, simulation, wireless, microstrip antenna, CST microwave studio.

LIST OF FIGURES

LIST OF TABLES

TABLE OF CONTENTS

CHAPTER 1
INTRODUCTION

1.1 INTRODUCTION

An antenna is a specific transducer which transforms radio frequency fields into alternating current and vice-versa. Electromagnetic energy in terms of waves is radiated or transmitted into the free space by the transmitting antenna; then the radio frequency travels through the free space and finally a part of this energy has been accrued by the receiving antenna. Antenna is acquiring huge changes from previously used wire antenna for broadcasting, communication link to the latest radar, missile, medical and defense application. The wideband mobile private communication having superior mobile video feature is everyone's need today.

Antenna will not be antiquated due to their absolute and strong principle; the change is only on the basis of technology which is changing every day. In 1970s, there was a tremendous advancement in the antenna due to the introduction of microstrip technology. In today's world, antenna, an essential portion of wireless devices, has endured renovations from a straightforward metallic rod to ceramic chip, adaptive, energetic and complex smart antenna. In the recent future, antenna will become a part of our nail with the advancement of nano-technology.

1.2 MICROSTRIP ANTENNA AND ITS DIFFERENT FEEDING TECHNIQUES

The basic form of microstrip antenna consists of a dielectric substrate, patch and ground plane. The basic requirements for designing a microstrip patch antenna are [1]

- Substrate characteristics
- Design and dimension of the patch
- Height of the substrate
- Resonant frequency
- Feeding technique

Dielectric substrate is an insulator which is the main part of microstrip antenna and offers mechanical strength to antenna [1]. Various types of dielectric substrates are used e.g. Benzocyclobutane, Duroid 6010, Nylon fabric, Rogrer 4350, RT-duroid, foam, FR-4 *etc*.

It is essential to excite the antenna for proper radiation and accordingly there must be proper feeding mechanism. There are different feeding mechanisms by which an antenna can be properly excited. The characteristics of different feeding mechanisms are concisely indexed in Table 1.1.

Table 1.1 Comparative studies between different feeding mechanisms of microstrip antenna [8]

Characteristics	Microstrip line feed	Coaxial feed	Aperture coupled feed	Proximity coupled feed	Coplanar Waveguide (CPW) feed
Structure	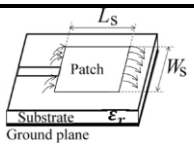	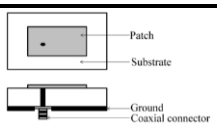	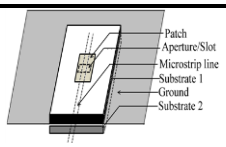	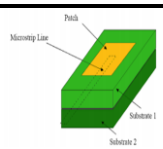	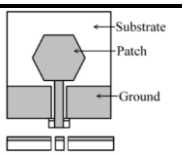
Fictitious feed radiation	More	More	Less	Minimum	Lesser
Authenticity	Better	Poor due to soldering	Good	Good	Decent
Ease of fabrication	Easy	Requirement of drilling and soldering	Alignment required	Alignment required	Alignment required
Impedance matching	Simple	Simple	Simple	Simple	Simple
Bandwidth	2–5%	2–5%	21%	13%	3%

1.3 UWB ANTENNA

Ultra-Wideband (UWB) is a band of frequency possessing pulse of very short duration. As per the definition of UWB, it is an wireless system possessing fractional bandwidth greater than 20% and a entire bandwidth more than 500 MHz. A UWB system is consisting of different desired achievements e.g. high data rate, more accurate ranging and lower price transceiver implementation *etc*. After a huge research work on ultra-wide band wireless communication, enormous numbers of utilizations have been detected in high speed short range wireless communication systems e.g. medical application, radar, military application, robotics, internet of things (IOT) and many other applications. The Federal Communication commission has

assigned a wide frequency band ranging 3.1–10.6 GHz for unlicensed ultra-wide band (UWB) having Equivalent Isotropic Radiated Power (EIRP) lower than -41.3dBm/MHz [2]. Antenna having wide range of frequency bandwidth and good radiation characteristics is required for performing this type of system [3].

It is very tedious job to design an antenna for such systems acting as band pass filter having wide bandwidth, superior gain, omni-directional radiation pattern, high radiation efficiency. But, different modified structure such as tapered patch, partial ground, tapered ground, CPW fed structure, stepped patch, stepped ground, slot loaded patch and ground, different meta-materials applied on patch, ground or on both can solve this problem. The design varieties are based mainly on the geometry of the radiating patch and location and as well as geometry of ground plane. Different UWB printed monopole antennas are shown in Figure 1.1. An impedance bandwidth of 2.3:1 to 3.8:1 can be attained by applying these antennas. Patches having different structures are used in these antennas e.g. simple circular monopole [4], octagonal monopole [5], spline-fashioned monopole [6], U-formed monopole [7], knight's wheel formed monopole [8] and two molded circular monopole [9].

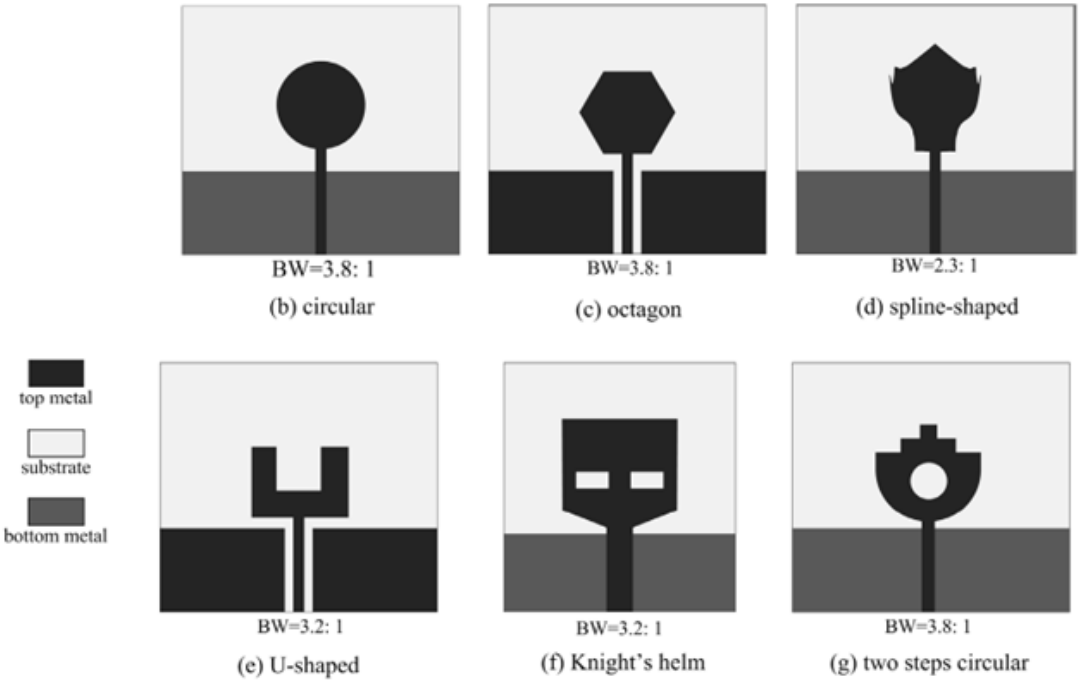

Figure 1.1 Various monopole UWB antennas [4–9]

1.3.1 Advantages of UWB

UWB acquires several advantages which are noted below:

- High data rate: UWB acquires frequency in GHz, as it is used in high frequency therefore it can achieve high data rate near to hundreds of Mb/s and the achievable range can be upto 10 meters.
- Minimum penetration loss: It works on both line-of-sights as well as nonline-of-sight surroundings. So it can penetrate through obstacles having a minimum loss.
- Fading hardiness: UWB system is exempted to multipath fading. As it has fading robustness characteristics, the complexity of transceiver may be reduced.
- Security: As UWB signal is very short duration pulses so its characteristics resemble with the characteristics of noise. Therefore it is secured system.
- Low cost: The complexity of UWB system is less; hence it is of low cost.
- Less power consumption. The power consumption by UWB system is less.

1.3.2 Importance of UWB

- The channel capacity of AWGN is bestowed by Shannon's theorem $C = B \log_2 (1+SNR)$ (1.1) where C is the capacity of channel in bits per second, B is the bandwidth of channel in Hz, and SNR is the signal-to-noise ratio.
- The capacity of channel can be raised by raising the signal at low bandwidth of the signal to noise ratio and hence the high data rate will also be uplifted.
- The output power of UWB system is less, in the range of milli Watt. Hence, low power transmitter can be used.

1.3.3 Drawbacks of UWB

- As the power limit of UWB system is less, therefore it can be operated up to 10 m at a rate of 100 Mbps.
- Other narrowband wireless standards e.g. WLAN, WiMAX, Aeronautical Radio Navigation band, ITU etc. can cause interference in UWB at the time of transmission. UWB antenna experiences interference due to the existence of different wireless standards. So various techniques are required to reject undesired frequencies.

1.3.4 Application of UWB Antenna

- High resolution radar: Detection and movement of objects near vehicle are more accurate.

- Wireless personal area network: UWB is an ideal technology to replace the wires of the personal computers and their peripherals, without interfering with the local wireless network.
- Military communication: The probability to detect UWB pulses is very low. Thus, the covert military communications are ideal for that purpose.
- Imaging system: UWB antenna can be applied in imaging systems, like ocean imaging, medical diagnostic, etc. UWB reflections from the target exhibit not only changes in amplitude and time shift, but also changes in the pulse shape.
- Emergency situation: UWB signals can penetrate obstacles because of the wide frequency spectrum. This property is very useful to detect and rescue survivors in disaster situations.

1.3.5 Different Techniques implied for Notching in UWB Antenna

- Etching various slots on UWB
- Electromagnetic band gap structures
- Stepped Impedance resonator
- Split ring resonator
- Complimentary split ring resonator
- Parasitic element.

In this work, planar monopole antennas incorporated with multiple types of band notching elements are designed, fabricated and tested for UWB applications which have band rejection criteria also.

1.4 MOTIVATION

In the last two generations, almost each and every field of human society has been captured by wireless technology. Pursuing the fast advancement of wireless terminals along with the increasing demand for recent services, cell phones offer a liberty so that communication between each other becomes very easy. Due to all these reasons, UWB technology as well as WLAN offers the proficiency and internet accessing facility apart from using the costly cables. As FCC has allotted the UWB frequency spectrum, there is a rising demand for miniaturized and cheap UWB antennas which can offer satisfactory and useful results. UWB systems must be of

minimum size such that they can be fitted with other transportable wireless appliances. In place of conventional radiators, planar antenna can provide a system having minimum volume. So, looking at the strategy, the main aim of this work is to design a microstrip compact monopole UWB antenna having desired band rejection capability as well as minimum volume. It becomes very difficult to achieve the ultra-wide band by a simple geometrical structural design. Compact structure of square and ellipse can give something broad bandwidth, but it should be modified further to get broader bandwidth. Bandwidth enhancement can be done beveling the patch. In this thesis, a spiked elliptical UWB antenna has been discussed in which the patch is having a compact design of square, ellipse and triangles to achieve ultra-wide band. The dimension of the feed line has been optimized for perfect impedance matching. Different types of slots and SRRs are implanted in patch, feed line and ground to get band rejection for undesired frequencies. Another miniaturized monopole UWB antenna has been proposed in this thesis, in which spikes have been appended to the partial ground and stepped patch has been offered to get ultra-wide band. The lowest part of the feed line has been extended to achieve proper impedance matching. Parasitic elements are implanted at the bottom portion of the substrate for getting band rejection.

1.5 PROBLEM STATEMENT, RESEARCH OBJECTIVE AND SCOPE

The problem statement of this thesis is to get a survey of UWB antenna having compact size and undesired band rejection capability. For this purpose, several UWB antennas having compact size and band notching characteristics have been studied and these are mentioned in literature review. Assembling all the inclusive knowledge about UWB antenna with different number of notches for different applications, the principal objectives were drawn as follows:

Research objectives:

- To design and simulate a CPW fed UWB antenna with five band notches.
  - Parametric study of notching element of the proposed antenna
  - Fabrication and testing of the proposed antenna
- To design and simulate a parasitic element loaded UWB antenna with three band notch.
  - Parametric study of notching element of the proposed antenna
  - Fabrication and testing of the proposed antenna

- To make a comparison between simulated and measured results of both the UWB antennas.

To achieve the aforesaid objectives, a number of problems have been studied and resolved. The problems are as follows:

- The effect of dimension of the slots on the notch frequency (Chapter 3)
- The effect of location and dimension of parasitic strips on the notch frequency (Chapter 4)

Scope:

A peculiar microwave design exercise comes with problem identify, initial design, effect of parametric variation on performance, optimization of the design, fabrication, testing and comparison with simulated result. First of all, various types of literatures are studied to start the research work.

The present research work highlights on UWB antenna possessing interfering band rejection capability. The UWB frequency range is 3.1–10.6. But, there also exist some narrow wireless frequency bands in this UWB range which are tabulated in Table 1.1. The UWB and existing wireless narrow bands are picturized in Figure 1.2.

Table 1.2 Wireless frequency bands and their application

Wireless Bands	**Frequency bands (GHz)**	**Bandwidth (GHz)**	**Application**
UWB	3.1–10.6	7.5	Radar, WPAN, military, imaging, etc.
WiMAX	3.3–3.7	0.4	Helps users to access present data, video, voice, mobile and internet access.
ARN	4.2–4.5	0.4	Used globally by the airborne radio altimeter for more than 40 years to improve safety and avoid Controlled Flight Into Terrain accidents.
WLAN	5.15–5.85	0.5	LAN extension, cross building interconnect, support nomadic access, ad hoc networking, etc.
ITU-8	7.9–8.8	0.9	For transport (long-haul), connections (including backhauling) in rural areas or to provide links to far offshore islands.
Amature radio band	10–10.5	0.5	allocated on a primary basis to the government radiolocation service, and on a secondary basis for non-government radiolocation services and the amateur radio service

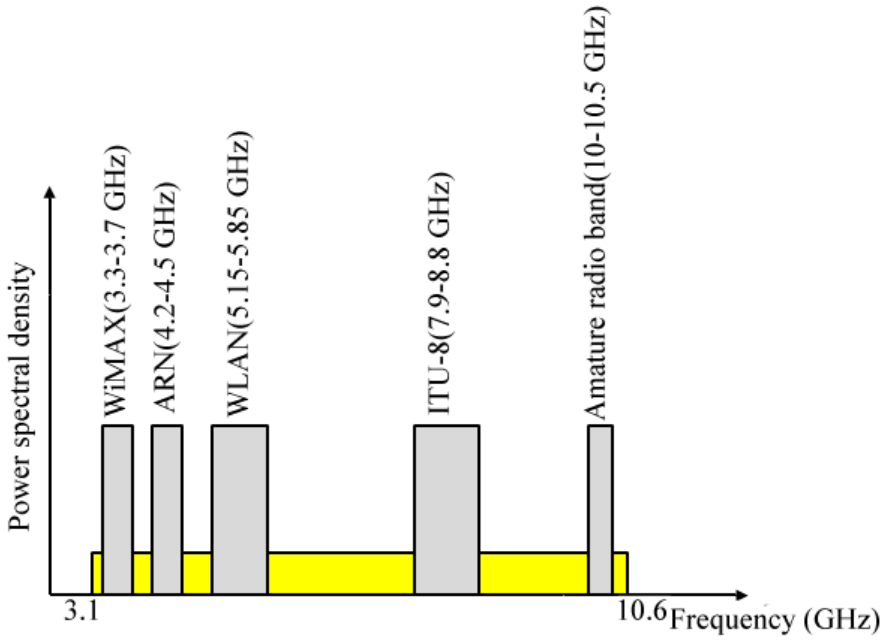

Figure 1.2 Ultra-wideband and co-existing narrow wireless bands

1.6 METHODOLOGY

- Comprehensive literature survey has been carried out in the field of UWB antenna having different number of band notches
- Effect of variation of antenna dimension on reflection coefficient, VSWR, gain
- CST MWS V14 has been used for doing the simulation of the proposed antenna
- Parametric study of different notching element is done using the in built "parametric sweep" option
- Both the antennas are fabricated on economical and easily available substrate "Fiber-glass epoxy" FR-4 material
- The reflection coefficient measurement has been performed using Agilent E5071C Vector Network Analyzer accessible at Antenna Research Laboratory, ECED in Thapar Institute of Engineering and Technology, Patiala
- The radiation pattern and gain of the proposed antenna gave been analyzed with the help of Anechoic chamber available at Millimeter Wave Laboratory, ECED in IIT, Roorkee
- For displaying and analyzing the plots of simulated and measured results, Origin version 6.2 has been used

1.7 ORGANIZATION OF THE WORK

Five chapters are included in this work. Overview of the various chapters is as follows: First chapter includes the introduction part along with fundamental of wireless system and brief introduction of antenna. Motivation and thesis objective is also included in this chapter. Literature review related to microstrip antenna, different feeding techniques, method of analysis, UWB antenna, different notching techniques incorporated in UWB antenna are included in the second chapter. Third chapter includes design, simulation, fabrication and testing of a compact monopole UWB antenna having five stop bands. Fourth chapter includes design, simulation and fabrication of a miniaturized monopole UWB antenna which has three stop bands. Conclusions and scope for future work are presented in the concluding chapter.

CHAPTER 2

LITERATURE REVIEW

2.1 INTRODUCTION

In today's world the wireless communication system has become an essential part of our life. Antennas are evaluated as an important and essential component in today's wireless communication system. According to the IEEE definition antenna is," *a mean for radiating or receiving radio waves*" [10]. In the transmitting mode the electromagnetic energy from the source reaches to the transmitting antenna after travelling through the transmission line, and then the antennas radiate the electromagnetic energy in the free space, whereas the receiving antenna accumulate a part of this radiated energy in the receiving mode. Antennas are used in various fields starting from regular use up to highly secured defense use; *e.g.* remote controlled toy, radio, remote controlled television and car, mobile phone, satellite communication, radar, missiles, medical treatment etc. Everyday new wireless gadgets are originating to make our life easier as well as very fast. The low profile antenna which can give reliable communication becomes more and more demanding due to its application in spacecraft and aircraft.

Microstrip antenna (MSA) is no doubt most radical and eminent antenna in today's communication world. It has so many advantages such as light weight, low cost, low profile, can be easily arranged in arrays, easy to fabricate, can be incorporated with another microstrip elements in monolithic application. This antenna can be easily ascended on satellites, missiles without any significant adaptations. The MSA can be directly printed on printed circuit board (PCB) which makes it more familiar in wireless communication system. Due to these advantages microstrip antennas are the most encouraging aspirant in UWB utilization. This type of antenna has minimum manufacturing cost, a low profile and can be easily incorporated with other parts of monolithic microwave integrate circuit (MMIC) for a communicating device [11, 12].

2.2 MICROSTRIP ANTENNA

In this section a concise analysis of MSAs, their feeding technique, model analysis, design variables are discussed.

2.2.1 Fundamental Structure of MSA

MSAs recognized significant consideration commencing in the 1970s, even though the concept of the MSA can be sketched to 1953 [13] and a patent in 1955 [14]. The MSA in its elementary structure is clearly depicted in Figure 2.1. Both the topmost and lowermost part consists of ultra-thin ($t \ll \lambda_0$, λ_0 is the wavelength in free space) metallic strip (usually copper) and the thickness of dielectric substrate is between $0.003\lambda_0$ and $0.05\lambda_0$ [1]. Generally the dielectric constant ε_r of the substrate lies between 2.2 and 12. Substrate with lower dielectric constant and more thickness offer better efficiency, larger bandwidth but at the same time the size of the antenna becomes larger [15]. Miniaturized antenna can be made of substrate with higher dielectric constant and lesser thickness but the antenna efficiency and bandwidth of the antenna will be decreased [15].

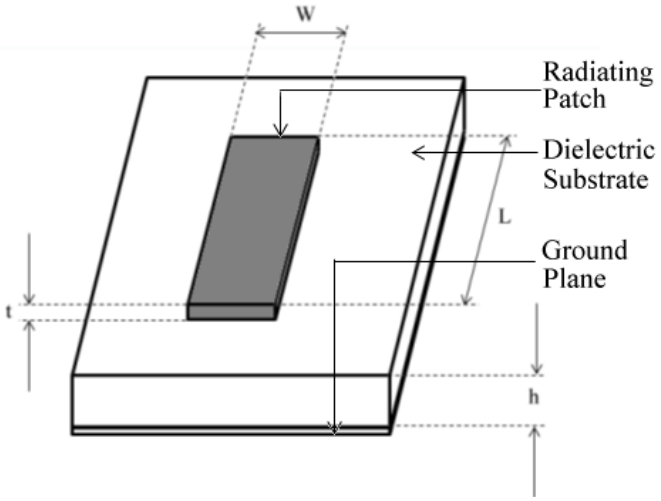

Figure 2.1 Geometrical structure of microstrip patch antenna

Usually MSAs are also acknowledged as patch antennas. The radiating patch and ground are photo-etched on the substrate. The radiating patch may be of different shapes such as rectangular, triangular, square, elliptical, circular ring, dipole and other compact shapes as shown in Figure 2.2.

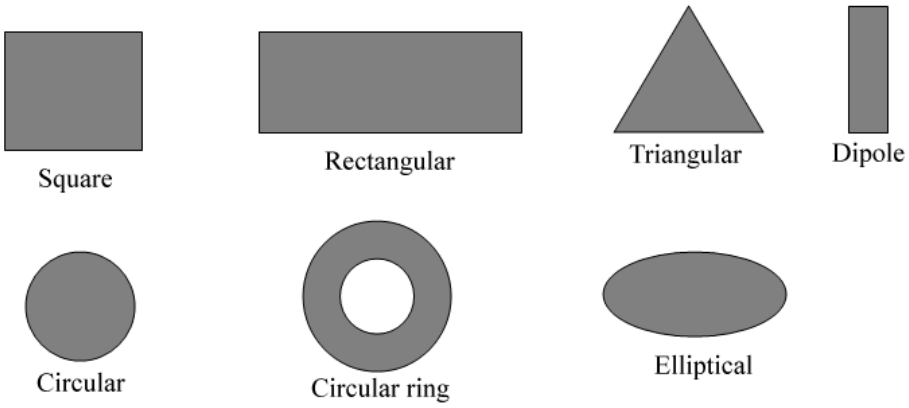

Figure 2.2 General shapes of microstrip patch elements

In case of rectangular patch, normally the length of patch L lies between $\lambda_0/2$ and$\lambda_0/3$. The patch has confined length and width, so a fringing field has been established along the patch rims. The amount of fringing depends upon the magnitude of patch length, width and substrate thickness. Due to this fringing field, the electrical length of the microstrip line has been decreased. Some waves penetrates through the dielectric substrate, at the same time some travel through air, due to this reason an effective dielectric constant ε_{eff} has been initiated to consider the fringing effect [1]. Hence, the MSA radiation is originated as a result of the fringing field generated between ground plane and patch. The dimension of the ground plane is associated with the thickness of the substrate. Normally the dimension of the ground plane is greater than the dimension of the patch by an amount of $\lambda_0/4$ approximately [7].

2.2.2 Feeding Technique

The method of deliver energy successfully to antenna from transmission line is known as feeding technique. The function of feeding technique is very important criteria for antenna input impedance matching. It plays a very important role to decrease the spurious radiation and broadening the impedance bandwidth, manages the surface wave, improving the radiation performance. There are various types of feeding techniques e.g. microstrip line feed, aperture couple feed, coaxial cable feed, proximity coupled feed and coplanar waveguide feed.

2.2.2.1 Microstrip Line Feed

In this type of feeding technique, a thin strip of same material and same thickness as that of the patch is connected to the edge of the radiating patch. It is a simplest feeding technique for impedance matching. In case of thicker dielectric substrate the spurious feed radiation and surface wave will increase which will in turn limits the bandwidth for practical design.

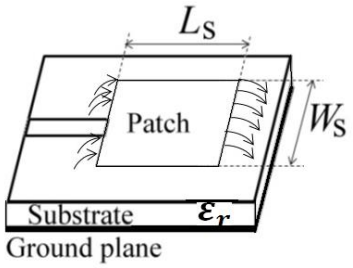

Figure 2.3 Microstrip line feed

2.2.2.2 Aperture Couple Feed

There are two types of substrates used in the aperture coupled feeding technique. The thin substrate with higher dielectric material placed at the bottom is separated by the ground plane from the thicker substrate with lower dielectric material as shown in Figure 2.4. The energy from the microstrip line, etched at the bottom of the lower substrate is coupled to the radiating patch, etched at the top of the upper substrate through a slot on the ground plane. In this type of feeding technique the feed line and the patch can be optimized separately. In this technique the interference of spurious radiation is minimized due to the isolation between feed line and radiating patch is done by the ground plane [1].

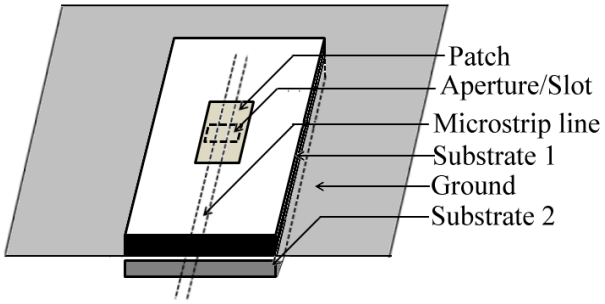

Figure 2.4 Aperture coupled feed

2.2.2.3 Coaxial Probe Feeding Technique

In case of coaxial probe feeding technique, the outer conductor of the coaxial cable is attached to the ground plane and the inner conductor elongates through the substrate and connected to the radiating element as shown in Figure 2.5. This technique has a significant advantage that it can be positioned at any craved place in the radiating patch for getting perfect impedance matching [1]. This technique has disadvantages of getting perfect dimension after drilling for the cable and a slim bandwidth [9].

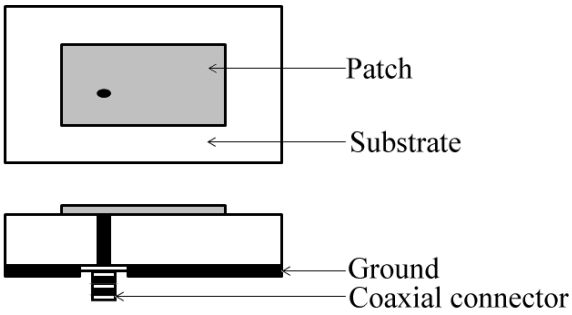

Figure 2.5 Coaxial feed

2.2.2.4 Proximity Coupled Feeding Technique

This technique is also recognized as electromagnetic coupling technique. Two types of substrates are used in this feeding technique also. The radiating patch is etched on the top of the upper substrate and the feed line is in between the two substrates as clearly depicted in Figure 2.6. This technique has an advantage of reducing spurious radiation but has a disadvantage bout the proper alignment of the two substrates.

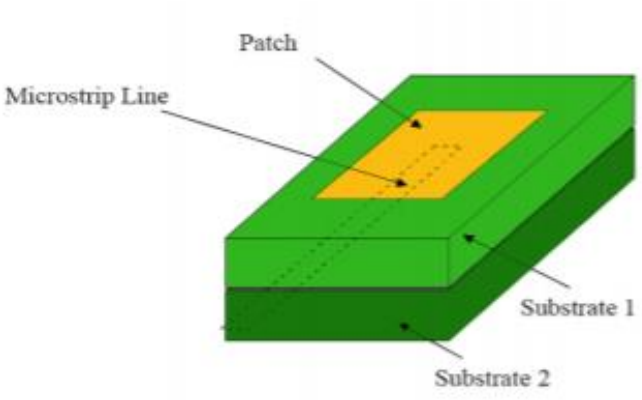

Figure 2.6 Proximity coupled feed [8]

2.2.2.5 Coplanar Waveguide Feeding Technique

Both the radiating patch and the ground plane are etched on the top of the dielectric substrate. A thin strip feed line is connected to the lower edge of the patch. Twin ground planes are laterally placed at the two sides of the feed line separated by a very little gap as shown in Figure 2.6. CPW (coplanar waveguide) was invented by Cheng P. Wen in 1969 [10]. There are many advantages of CPW e.g. radiating patch and ground plane are etched on the same side of the substrate, light weight, low radiation loss, can achieve broader bandwidth [11].

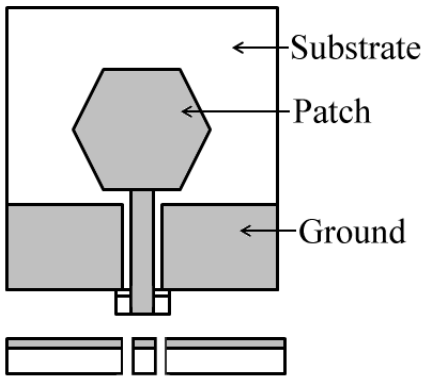

Figure 2.7 Coplanar Waveguide feed

Recently, numerous CPW-driven monopole antennas have been commenced for UWB antennas due to its humble structure, ease of fabrication, less cost, broader impedance bandwidth.

2.2.3 Methods of Analysis

Method of analysis of MSA is important to predict the antenna gain, polarization, radiation efficiency, input impedance, frequency bandwidth. A good and efficient model helps to calculate all the antenna radiation and impedance characteristics. There are mainly three types of method e.g. transmission line model, cavity model and full wave model. MSAs are computed and assessed by employing any one of the three models.

2.2.3.1 Transmission Line Model

This model is the easiest one among those three models but at the same time it has the least accuracy. This model illustrates the MSA model by two slots of height *h* and width *W* isolated by a low impedance transmission line whose length is *L*. As the width and length of the MSA

are confined, there is a fringing effect created at the edge fields which is clearly depicted in Figure 2.7. The measure of fringing relies on the thickness of the substrate and the dimensions of the radiating patch.

The fringing influences the resonant frequency of the microstrip patch antenna, so it must be taken in to account in to the microstrip patch antennas calculation. The fringing effect plays an important role at the time of microstrip patch antenna calculations due to its control over the antenna resonance frequency. It can be clearly visualized from the Figure 2.7 that, maximum field lines stay in the dielectric substrate whereas a few lines dwell in the air, as a result the electrical dimension of the microstrip line becomes broader as compared to its physical dimension. So the phase velocity in substrate and air will be different and as a result the transmission will be quasi TEM (transverse electromagnetic) instead of TEM. Accordingly an effective dielectric constant must be calculated to elucidate the fringing effect which is denoted as ε_{reff}.

$$\varepsilon_{reff} = \frac{\varepsilon_r+1}{2} + \frac{\varepsilon_r-1}{2}\left[1+\frac{12h}{W}\right]^{-1/2} \quad (2.1)$$

Where ε_r = dielectric constant of the substrate, h = height of the substrate and W= width of the patch.

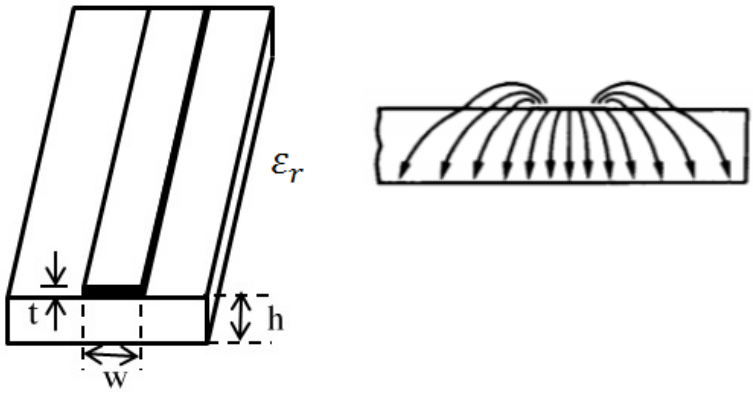

Figure 2.8 Transmission line model

In case of a microstrip patch antenna working in its basic TM_{10} mode, the patch length should be little less than the half of the wavelength in the dielectric medium. MSA can be figured as a two end open structure with two slots segregated by an L length transmission line as clearly depicted in Figure 2.8. Due to the open ended structure, there is a maximum voltage and

minimum current along the breadth of the patch. The fields at the concluding edges can be resolute into perpendicular and digressive components about the ground plane.

As shown in Figure 2.9, the direction of the electric field perpendicular component at the two verges along the breadth is opposite to each other and they are out of phase also. They cancel each other along the broadside length as the length is $\lambda/2$.

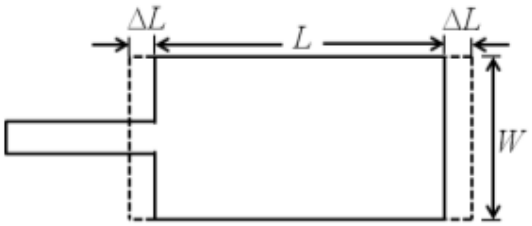

Figure 2.9 Original physical length and effective length as a result of fringing effect

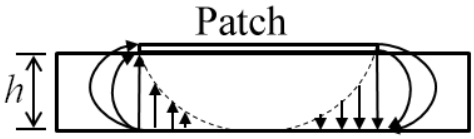

Figure 2.10 Side view of microstrip antenna

The resulting fields due to in phase digressive components merge; as a result the maximum radiated field is achieved which is perpendicular to the surface of the antenna. Therefore the edges by the breadth may be delineated as two radiating slots, which are separated by half the wavelength. The fringing fields may be formed as radiating slots and the electrical dimension of the patch becomes larger than the physical dimension. The patch length dimension increases as an amount of ΔL, which depends on effective dielectric constant and the ratio width: height of the substrate. The magnitude of the extended length, ΔL can be calculated by the equation given by Hammerstad [12]

$$\Delta L = 0.412h\frac{(\varepsilon_{reff}+0.3)+\left(\frac{W}{h}+0.264\right)}{(\varepsilon_{reff}-0258)+\left(\frac{W}{h}+0.8\right)} \tag{2.2}$$

The operative length of the patch becomes

$$L_{eff} = L + 2\Delta L \tag{2.3}$$

The relation between bestowed resonance frequency f_0 and L_{eff} is given as

$$L_{eff} = \frac{c_0}{2f_0\sqrt{\varepsilon_{reff}}} \tag{2.4}$$

For any T_{mn} mode, the resonance frequency of a rectangular MSA f_0 is given by James and Hall[3]:

$$L_{eff} = \frac{c_0}{2\sqrt{\varepsilon_{reff}}}\left[\left(\frac{m}{L}\right)^2 + \left(\frac{n}{W}\right)^2\right]^{1/2} \quad (2.5)$$

Where *m* and *n* are the modes of the antenna along the length and width of the patch. In case of a skilled antenna, the useful width of antenna *W* is given by [13]:

$$W=\frac{c}{2f_r}\sqrt{\frac{2}{(\varepsilon_r+1)}} \quad (2.6)$$

2.2.3.2 Cavity Model

Transmission line model has several disadvantages such as; it is beneficial only for rectangular patch antenna and also it overlook the field variation along the radiating edge. Cavity model has overcome this problem. The inner quarter of the substrate is formed as a cavity confined by magnetic wall by the sides and by electric walls at base and top. As the thickness of the substrate is very less, therefore the interior electric field characteristics remain almost same in the *Z* direction. The magnetic field is transverse one and it has two components$H_x and\ H_y$. When the patch is exited, dispersion of charges has been noticed at the base and top of the patch and at the lowest part of the substrate as clearly depicted in Figure 2.11. The dispersion of charge has been controlled by two mechanisms e.g. attractive and repulsive. The attractive mechanism works between the opposite charges at top of the ground plane and lower side of the patch and this supports maintaining the entire charge condensation at the bottom of the patch. As the name suggests, the repulsive mechanism takes place between identical charges at the bottom and topmost side of the patch. As a result of this repulsion, few charges are moved from bottom to the topmost side of the patch and consequently there is a flow of current. As per the assumption of cavity model,$h/W \ll 1$. Due to this reason the repulsion mechanism remains suppressed over the dominance of attraction mechanism and most of both the charge distribution and current remain at the bottom of the patch. A little amount of current flows through the upper surface and it becomes approximately equal to zero as the value of h/W decreases more. Therefore no tangential magnetic component will be created at the patch edges. Accordingly, patch sidewalls can be postured as perfect magnetic conducting surface. From the above discussion it can be concluded that the dielectric field distribution underneath the patch will not be dispersed. Practically, the value of h/W should be finite which will not force to make the tangential magnetic field to be zero. But as the tangential magnetic field is very small, four wall of the

patch could be estimated as perfectly magnetic acting. There will be complex pole in the impedance function of the MSA. The imaginary part of the poles is due to the radiation power loss, conduction loss and dielectric loss. Since the four walls and the inner substance are lossless, the cavity will be non-radiating in nature and accordingly there will be totally reactive input impedance.

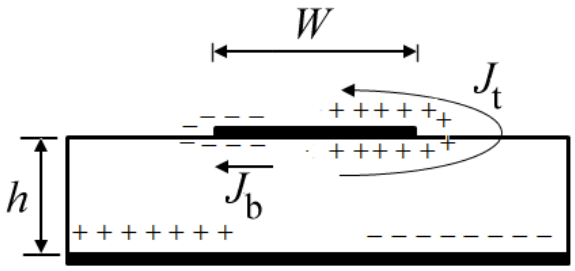

Figure 2.11 Distribution of charge and formation of charge density on the microstrip patch

So, for adequate radiation, the cavity should be considered as lossy in nature and the value of effective loss tangent

$$\delta_{eff} = 1/Q_T \tag{2.7}$$

Where Q_T = Quality factor of antenna

$$\frac{1}{Q_T} = \frac{1}{Q_d} + \frac{1}{Q_c} + \frac{1}{Q_r} \tag{2.8}$$

Where Q_d the quality factor of the dielectric is expressed as

$$Q_d = \frac{\omega_r W_T}{P_d} = \frac{1}{tan\delta} \tag{2.9}$$

Where ω_r=angular resonance frequency

W_T=total stored energy in the patch

P_d =dielectric loss

Q_c , the quality factor of the conductor is expressed as

$$Q_c = \frac{\omega_r W_T}{P_c} = \frac{h}{\Delta} \tag{2.10}$$

Where P_c= loss in conductor

Δ=skin depth of the conductor

h=substrate height

Q_r , the quality factor for radiation is expressed as

$$Q_r = \frac{\omega_r W_T}{P_r} \quad (2.11)$$

Where P_r is the radiated power from the patch.

By replacing the equations (2.9), (2.10) and (2.11) in (2.7) we achieve

$$\delta_{eff} = tan\delta + \frac{\Delta}{h} + \frac{P_r}{\omega_r W_T} \quad (2.12)$$

The effectual tangent loss of the antenna is explained in Equation (2.12). If the value of *Q* is recognized, the antenna can be studied due to its lossy nature.

2.2.3.3 Full Wave Solution Method

In this method MSA are modelled by employing surface current and the simulation of the dielectric substrate is done by employing the volume polarization current. An integral equation is fetched for the aforesaid unusual currents are revealed by Newman and Tulyathan [14] and Harrington [15] and they are expressed in a matrix form using this integral equation. Therefore, by using any of the aforesaid algebraic equation, the value of current and different other parameters e.g. the dispersed electric and magnetic field can be calculated instantly. Hence, antenna problem also can be solved by utilizing the aforesaid integral equations.

2.3 UWB ANTENNA

On the basis of the rules of Federal Communications Commission (FCC), an unlicensed large frequency band of bandwidth 3.1–10.6 GHz has been declared named as ultra-wide band as per its characteristics. There are various advantages of ultra-wide band antennas which make them fascinating and attractive. They offer exceptionally high data rate and their power consumption is very less [16]. There is huge application of UWB antenna due to the large bandwidth [17].

2.3.1 History

UWB antenna was first presented as square plate dipole, spherical dipole, triangular or bow-tie dipole and biconical dipole by Oliver Lodge in 1898 which are accurately used as transmit-receive link [18]. After that a huge research and development has been done in UWB antenna.

In conjunction with miniaturization of wireless technology and the increment of operating frequency, various new types of omni-directional UWB antennas specially UWB planar monopole antenna and UWB printed monopole antenna has been made in last decade. Both the aforesaid types are evolved from the traditional UWB antennas, for instance cage antenna, biconical antenna, etc. The new types of unconventional antennas provide approximately the

same bandwidth improvement, omni-directional radiation pattern as the conventional UWB antennas but with an advancement of size reduction.

2.3.2 UWB Printed Monopole Antenna

Normally, UWB printed monopole antenna consists of a dielectric substrate, a patch printed or itched on top of the substrate, a ground plane itched on top or bottom or on both of the substrate and a microstrip feed line or CPW feeding technique for energizing the antenna. After Choi *et al.* [19–20] has presented this type of wideband antenna, numerous printed monopole antennas are designed in the succeeding years.

As clearly depicted in Figure 2.12, a CPW fed UWB monopole antenna has been reported in which the impedance bandwidth is 2.9–18 GHz [27]. The patch of the antenna is specially modified octagonal shape. It can be noticed that the optimized impedance matching can be achieved by adjusting the feed width.

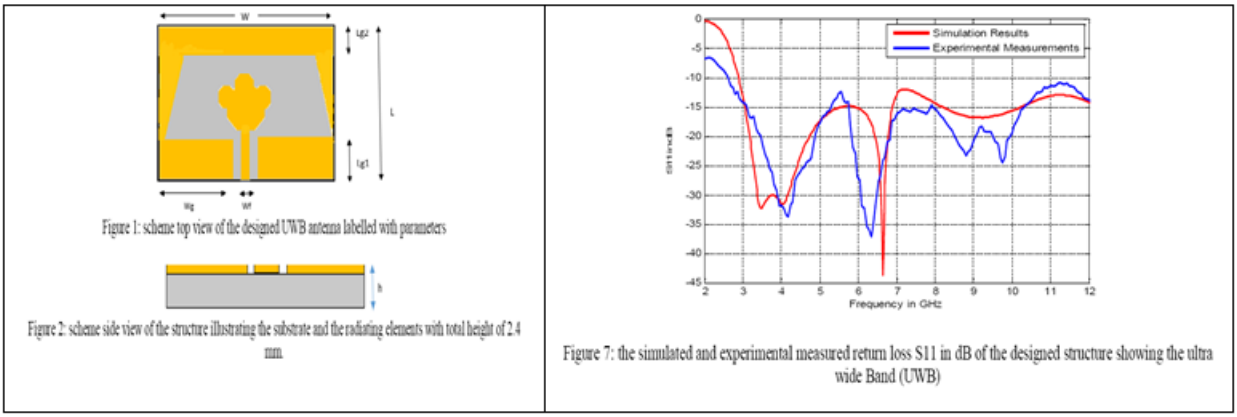

Figure 1: scheme top view of the designed UWB antenna labelled with parameters

Figure 2: scheme side view of the structure illustrating the substrate and the radiating elements with total height of 2.4 mm.

Figure 7: the simulated and experimental measured return loss S11 in dB of the designed structure showing the ultra wide Band (UWB)

Figure 2.12 CPW fed octagonal UWB antenna [27]

In recent years, metamaterials are applied to posture antenna having substrate with low permettivity for size reduction, better gain, enhanced as well as broader bandwidth. A metamaterial based UWB antenna has been stated by G. K. Pandey *et al.*[28] which has a compact size of 27.6×30.8 mm^2 , a high average gain of 4dBi and a wide banndwidth which is shown in Figure 2.13.

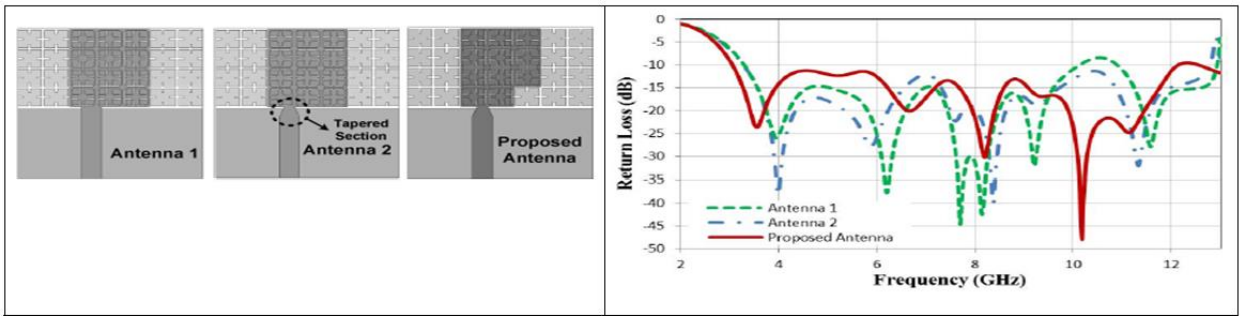

Figure 2.13 Metamaterial based UWB antenna [28]

2.3.3 Band Notched UWB Antenna

FCC has declared the UWB bandwidth as from 3.1–10.6 GHz, but some narrow frequency bands also prevail in this frequency band. Due to this coexistence, it may cause interference. To overcome this type of interference, those narrow frequency bands should be rejected and accordingly some band notching techniques e.g. implanting slots, parasitic element, hybrid technology, etc. should be applied.

2.3.3.1 Implanting Slots and SRRs

In between all the band notching, implanting slots is easiest technique. As shown in Figure 2.14, a slot loaded CPW fed compact rectangular UWB antenna has been stated in which one single horizontal slot at the top and two symmetrical vertical slots at the two sides on the radiating patch are etched to get band rejection at X band uplink and downlink satellite communication respectively [29].

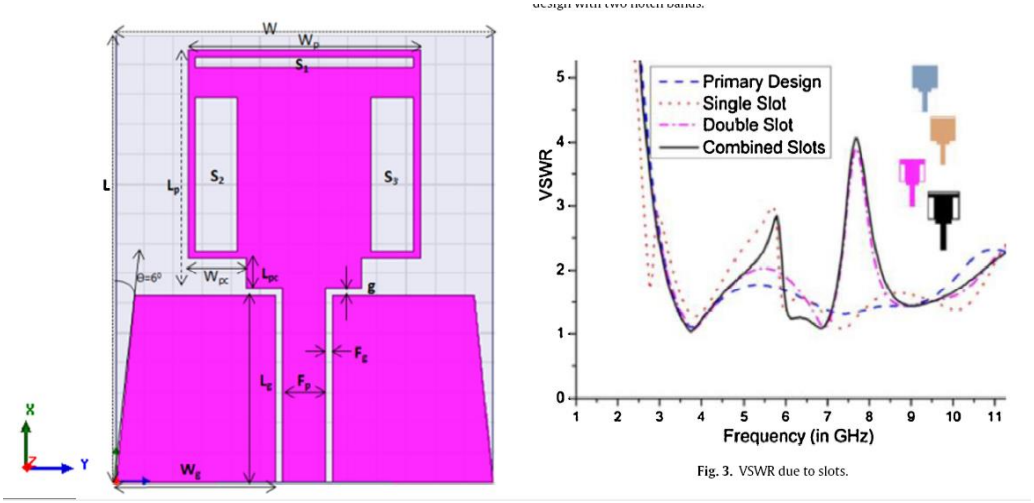

Figure 2.14 Slot loaded rectangular UWB antenna structure and its VSWR response

A CPW fed circular patch antenna has been reported [30] in which three single SRRs are applied on the bottom of the dielectric substrate to get three band rejections at WiMAX, WLAN and X band satellite communication centered at 3.5, 5.5 and 7.9 GHz respectively as clearly depicted in Figure 2.15.

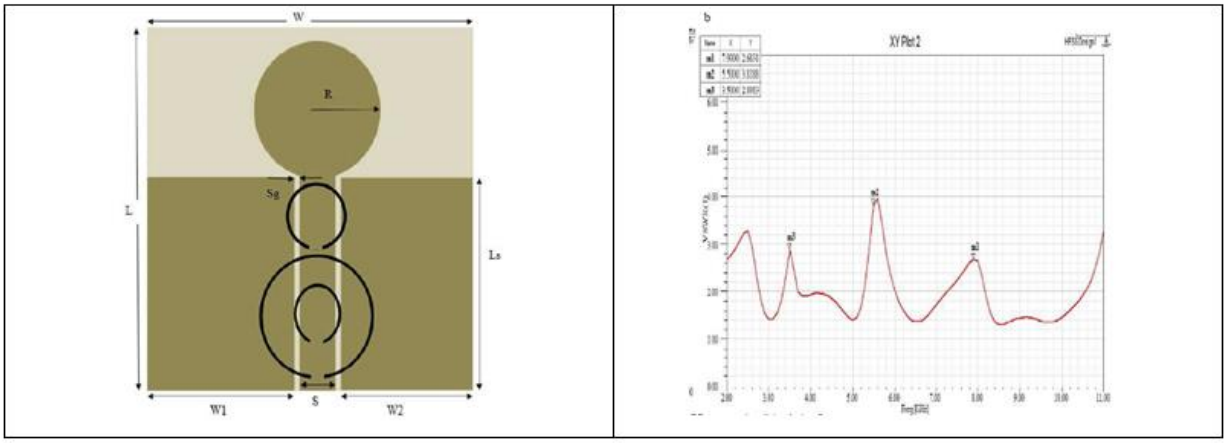

Figure 2.15 Top view and VSWR response of three single SRR loaded UWB antenna [29]

2.3.3.2 Parasitic Element

Much like embedding slots, parasitic elements are also applied for getting band rejection. A planar monopole UWB antenna having circular radiating patch and partial ground has been reported [30] in which a pair of parasitic strips are applied near to the radiating patch to reject 5–6 GHz band and a pair of slots are etched on the ground to reject WiMAX band as shown in Figure 2.16.

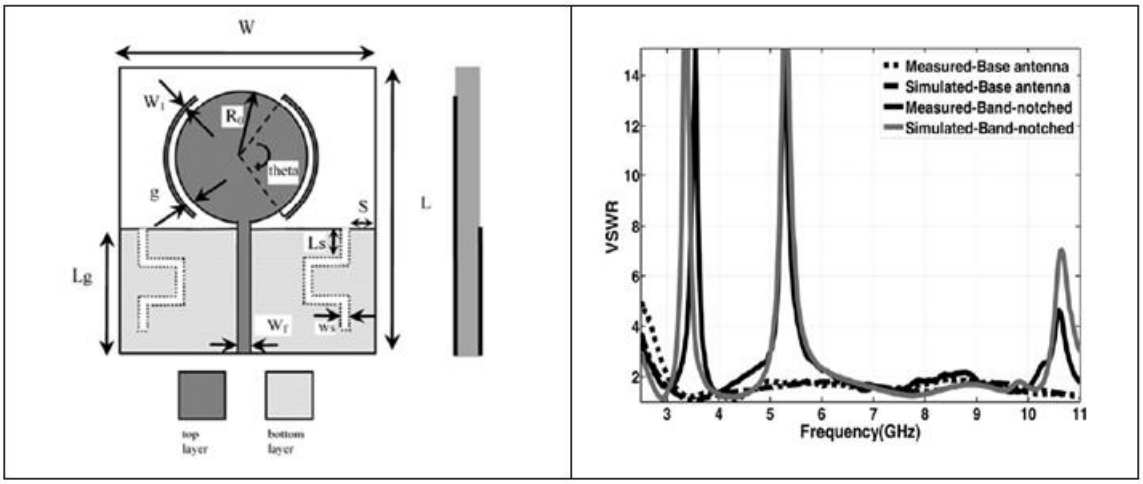

Figure 2.16 Structure and VSWR response of a circular monopole UWB antenna with parasitic element for band rejection [30]

A half circular shaped UWB monopole antenna has been stated [31] in which three pairs of parallel parasitic elements with tapered at both ends are applied on both sides of the feed line to get three band notches as clearly depicted in Figure 2.17.

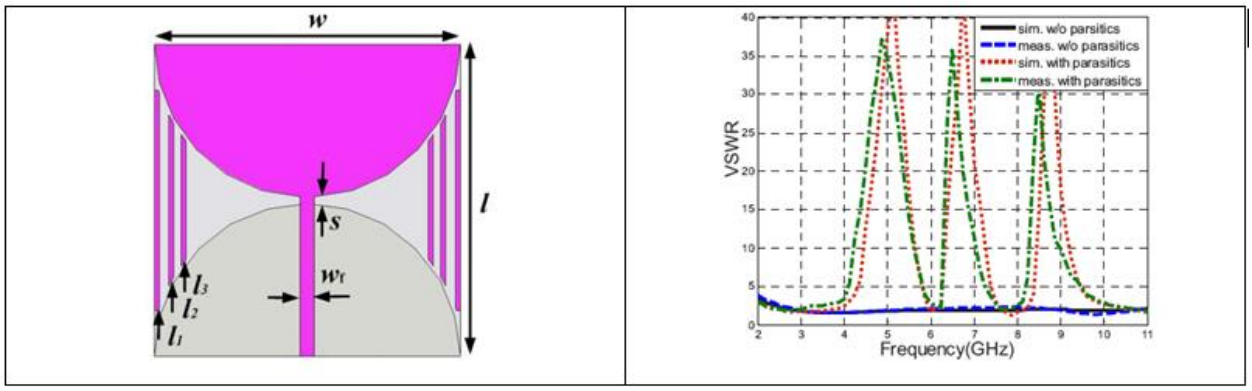

Figure 2.17 Structure and VSWR response of a parasitic element loaded half circular UWB antenna having three stop bands [31]

2.4 SOME RELEVANT DEVELOPMENTS IN NOTCHED UWB ANTENNAS

As the combination of various wireless applications, large bandwidth requirements and at the same time avoiding interference on a single device, notched UWB antenna is the perfect solution providing the overall size of the antenna as small as possible. In this section, an overview has been delivered on some recent developments in band notched UWB microstrip antennas.

S. H. Choi et al. (2003) proposed a rectangular patch antenna for UWB application. The antenna has a dimension of $30\times35mm^2$. Two steps and a slot on the radiating patch and a partial ground plane are applied to get perfect impedance matching and wide bandwidth of 3.2–12 GHz. The antenna has an overall gain of 5 dBi [23].

A Kumar and M.M. Sharma (2014) has presented an extremely wideband UWB antenna having double circular patch. A partial ground plane with both end beveled is applied at the bottom of the substrate. It has been noticed that the gap between ground and patch are very important for perfect impedance matching leading to a wide bandwidth. A small size SRR is applied on the lower portion of the radiating patch to get a band rejection for WLAN [35].

M. M. Islam et al. (2014) proposed a compact UWB antenna having single band rejection characteristics. A rectangular slot is cut out from the partial ground for impedance matching and hence wider bandwidth of 3.45 to more than 12 GHz. Two rectangular complementary split ring

resonators (CSRR) are implanted at the middle part of the patch to get a band rejection at 5.5 GHz. The magnitude of rejected frequency depends on the position of the CSRR [36].

R. K. Saraswat et al. (2014) presented an UWB antenna with triple band notch characteristics. Both the patch and ground are beveled to get wider bandwidth. One elliptical single SRR and two square SRR with different dimensions are applied on the patch to get three band notches at WLN, WiMAX and X band. The realized peak gain of the antenna is 3.98 dBi and the average gain of the UWB antenna is 2.55 dBi [37].

A. Bhattacharya et al(2017) presented a miniaturized UWB antenna of dimension 12×18 mm^2 has been proposed in which three bands have been rejected by applying parasitic element at the back side of the antenna. The thickness of the parasitic element is very thin for which the fabrication becomes a very tedious job [38].

X. J. Liao et al (2011) proposed an aperture coupled UWB antenna of dimensions of 24 × 30 mm^2 in which two bands viz. WLAN and WiMAX have been rejected by using three resonators [39].

Z. Wang et al(2016) presented a mushroom structured antenna having a dimension of 30×30 mm^2 has been reported in which parasitic circular arc-shaped structure, inverted L-shaped slot and asymmetrical structure along the feed line are embedded to reject WiMAX, WLAN and ITU bands respectively. But this antenna is unable to satisfy UWB gain characteristics because the value of gain at all the notched frequencies is positive and is greater than equal to 1 dBi. Further the gain plot for basic UWB antenna has not been shown which limits the comparative analysis between the original UWB antenna and the proposed notched UWB antenna [40].

I. B. Vendik et al (2017) proposed a CPW fed planar antenna having a dimension of 50×50 mm^2 has been reported in which ERR (electrical ring resonator) beneath the CPW has been embedded for rejecting WiMAX, WLAN and 7.5 GHz bands [41].

S. U. Rehman et al (2017) stated a CPW fed UWB antenna in which two pairs of DGS resonators are used. This antenna having a dimension 70×80 mm^2, to reject 2.5/3.5 GHz WiMAX, 802.11a WLAN, ITU-8 band. But both these antennas have the limitation of large size [42]. .

M. M. Sharma et al (2014) proposed a compact monopole UWB antenna of dimension 34×40 mm^2 has been reported in which four band notches have been achieved by using C and U shaped slots. In this particular paper the WLAN band has not been completely notched as it

rejects only the frequencies between 5.45-5.98 and thus interference exists in UWB antenna because of 5.15-5.45 bands [43].

T. Li et al (2012) presented a 35×44 mm^2 circular patch coplanar waveguide fed monopole antenna has been proposed in which four band notches have been achieved by using two circular split ring slots in the patch and two L-shaped slots in the ground. But the value of gain for basic UWB antenna is of the order of 4 dBi which is less than the gain values reported in recent literatures [44].

A. Kaur and G. Srivastava (2016) proposed a CPW fed UWB antenna has been reported in which four band notches have been achieved by applying double open circuited stubs and embedding slot resonator in the feed line. But the antenna again is of very large size of the order of 44×40.4 mm^2 [45].

Y. Jin et al (2016) stated a quadruple notched trapezoid UWB antenna has been proposed in which band notches are achieved by using different slots and CSRR (complementary split ring resonator). The size of the antenna is 30×33.5 mm^2 i.e. not miniaturized and thicknesses of the slots are very less which becomes imperfect at the time of fabrication [46].

2.5 OBSERVATIONS FROM LITERATURE REVIEW

After the broad literature review of various research papers and books, it has been perceived that several research works has been done in the field of UWB antenna possessing band rejection characteristics. Under the systematic study, it has been observed that various UWB antenna has been designed. Researchers have been developed different UWB antennas having different numbers of stop bands, but there are some fields that researchers studied insignificantly.

- Very few literatures are available in which more than four narrow wireless bands have been rejected.
- Very few literatures are available in which single composite parasitic element has been implemented to reject multiple bands.

2.6 RESEARCH OBJECTIVES

The principal objectives were drawn as follows:

Research objectives:

- To design and simulate a CPW fed UWB antenna with five band notches.
  - Parametric study of notching element of the proposed antenna
  - Fabrication and testing of the proposed antenna
- To design and simulate a parasitic element loaded UWB antenna with three band notch.
  - Parametric study of notching element of the proposed antenna
  - Fabrication and testing of the proposed antenna
- To make a comparison between simulated and measured results of both the UWB antennas.

To achieve the aforesaid objectives, a number of problems have been studied and resolved. The problems are as follows:

- The effect of dimension of the slots on the notch frequency (Chapter 3)
- The effect of location and dimension of parasitic strips on the notch frequency (Chapter 4)

CHAPTER 3

A COMPACT MONOPOLE UWB ANTENNA WITH SPIKED ELLIPTICAL RADIATOR

3.1 INTRODUCTION

In this chapter, a design of compact CPW fed monopole ultra-wide band antenna with five stop bands has been discussed. An inverted arc is placed on the top portion of modified elliptical patch so as to form a band notch for WiMAX (wireless interoperability for microwave access). A single ring SRR (split ring resonator) has been embedded at the center of radiating patch so as to achieve a band notch for ARN (aeronautical radio navigation). Two symmetrical slits have been etched in the ground thus forming DGS (defected ground structure) to get a band notch for WLAN (wireless local area network). Two concentric rectangular SRRs are etched from the feed line to obtain a higher frequency band notch for ITU-8 (International Telecommunication Union). Two symmetrical circular SRRs are etched from the lower portion of the patch near the feeding arrangement to obtain a band notch for Amateur Radio band. The simulation is carried out by using three-dimensional electromagnetic simulation software Computer Simulation Technology Microwave Studio Version 2014 (CST MWS V14.0) [18]. The proposed monopole UWB antenna with modified elliptical radiator having five band rejection features is fabricated and tested for its validation with simulated results. This chapter is organized as basic UWB antenna design, individual band notching technique, return loss, voltage standing wave ratio, parametric sweep analysis of notching elements, current distribution, gain and radiation pattern analysis. Finally, a comparison between simulated and measured results is inferred which validates the practical feasibility of the proposed structure.

3.2 ANTENNA DESIGN

The geometrical configuration of proposed UWB antenna with modified elliptical radiator with five band notched characteristics is shown in Figure 3.1. This antenna consists of two layers. The bottom layer is a substrate, made of dielectric material FR-4 (Flame Retardant-Fiber Glass Epoxy), the most popular inexpensive material to manufacture circuit boards, having relative permittivity (ε_r) 4.4, tangent loss (tan δ) 0.02 and thickness 1.6 mm. Both the patch and ground are made of PEC (Perfect Electric Conductor) and are at the top layer printed on the substrate with a thickness 0.035 mm. Microstrip line with width 3.6 mm is used to feed the spiked elliptical monopole UWB antenna to match impedance of 50 Ω. The proposed antenna has an

overall dimension of $29 \times 24 \times 1.6\ \text{mm}^3$. The design simulation is carried out using three-dimensional electromagnetic simulation software Computer Simulation Technology Microwave Studio Version 2014 (CST MWS V14.0). The optimization of proposed antenna is carried out by using parameter sweep Eigen mode solver window. The fabricated antenna prototype is shown in Figure 3.2. The basic UWB antenna exhibits a simulated impedance bandwidth of 2.87 GHz to 16 GHz with five band notching characteristics for WiMAX (3.3–3.7 GHz), ARN band (4.2–4.5 GHz), WLAN (5.15–5.85 GHz), ITU-8 band (7.9–8.5 GHz) and Amateur Radio Band (10–10.5 GHz). The feed line width has been designed to match characteristic impedance of 50 Ω using the following equations [19]:

$$\varepsilon_{eff} = 0.5(\varepsilon_r + 1) + \frac{0.5(\varepsilon_r - 1)}{\sqrt{(1+\frac{12h}{w_f})}} \tag{3.1}$$

$$Z_0 = \frac{120\pi}{\sqrt{\varepsilon_{eff}}[\frac{w_f}{h}+1.39+0.67\ln(\frac{w_f}{h}+1.44)]} \tag{3.2}$$

Where Z_0 is the characteristic impedance, ε_{eff} is effective permittivity of the substrate, w_f is feed line width and is h substrate height.

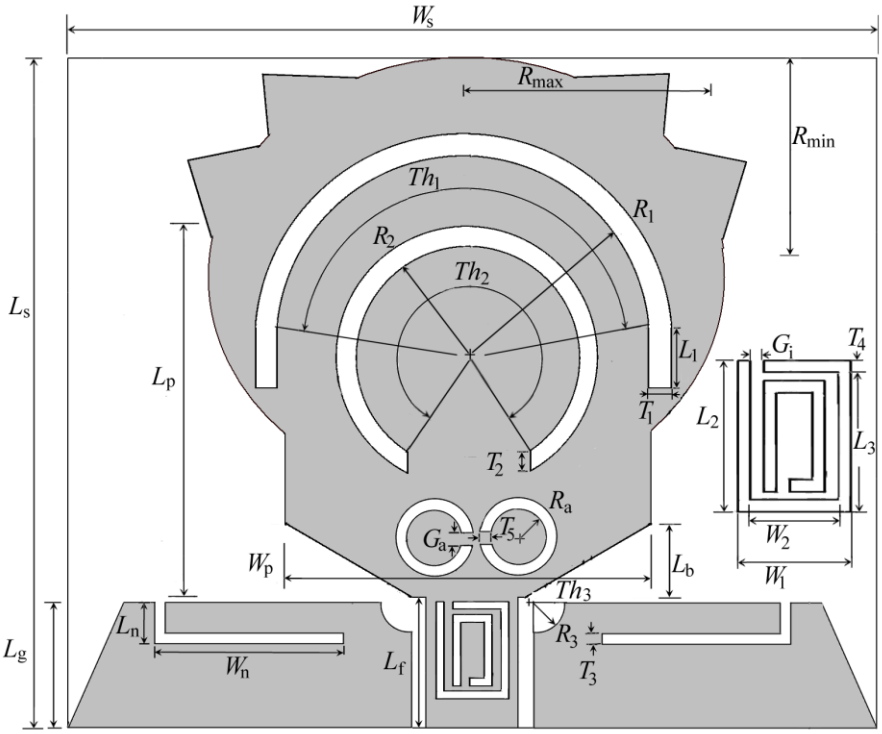

Figure 3.1 Top view of proposed UWB antenna with five band-rejection features

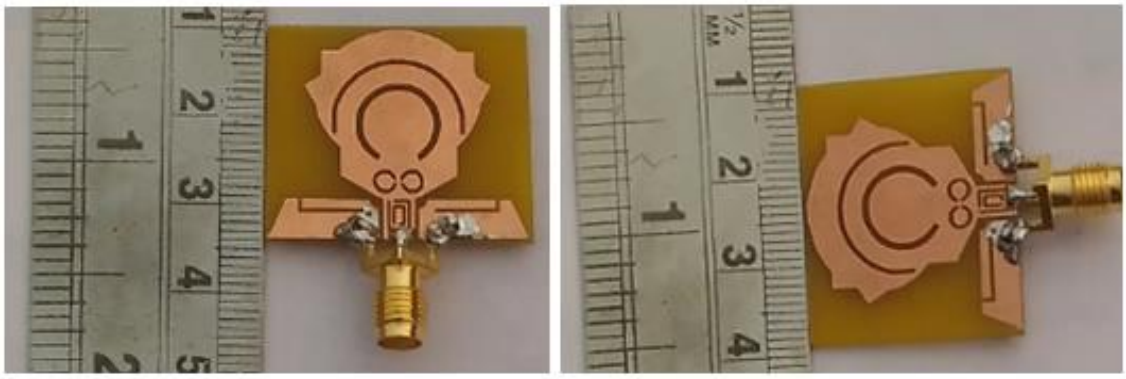

Figure 3.2 Fabrication of proposed UWB antenna

3.3 STEP-BY STEP APPROACH TO PROPOSED ANTENNA EVOLUTION

3.3.1 Basic UWB Antenna Design

Figure 3.3(a–c) shows step by step evolution of the basic UWB antenna. Initially the antenna had been designed as a square patch CPW fed monopole antenna having dimensions $13 \times 13\ \text{mm}^2$ and the ground was modified to a reduced ground plane with two symmetrical rectangular structures placed at both sides of the feed line as shown in Figure 3.3(a). But this antenna exhibits only one resonance band of 4.5–6 GHz as shown in Figure 3.4. This initial antenna is then modified and optimized to get a wide impedance bandwidth. In the first modification stage, three resonance bands *e.g.* 4 GHz, 7.38 GHz and 10.8 GHz ranging from 3.35–5.6, 5.8–8.5 and 9.2–14.3 GHz respectively have been achieved by beveling both the outer corners of the ground and lower corners of the square patch and ingraining an ellipse at the top of the patch as shown in Figure 3.3(b). In the final modification stage, two quadrants close to the feed point have been carved at the two inner corners of the ground plane and two adjacent triangles have been ingrained at both ends of the elliptical patch thus forming spikes at the top of elliptical radiator to enhance the bandwidth, as shown in Figure 3.3(c). After the final modification, an impedance bandwidth of 3.2–13.1 covering the whole UWB range has been achieved with four resonance frequencies viz. 4 GHz, 7.5 GHz, 9.9 GHz and 12 GHz which is very clearly depicted in Figure 3.4. This step by step improvement of the bandwidth can be more clearly understood from the Figure 3.5(a–d), in which the surface current distribution of the basic UWB antenna at four resonance frequencies has been shown. The fundamental mode has been created at 4 GHz as depicted in Figure 3.5(a), having the direction of current along *Y*-direction. It can be recognized from the current distribution shown in Figure 3.5(b) that the

second resonance mode or the first harmonic of fundamental mode has been created near about at 7.5 GHz, having surface current direction in the middle of the patch along with the topmost portion of the patch. As visualized from the Figure 3.5(c), third resonance mode or second harmonic mode has been produced at 9.9 GHz, having two extra outgoing current directions along with the first one. As clearly depicted in Figure 3.5(d), fourth resonance mode *i.e.* third harmonic mode has been formed at 12 GHz having three extra outgoing current direction along with the first one. As frequency increases, less current concentration at the radiating patch, more complicated current distribution at the edges of ground plane adjacent to the patch, are observed. Therefore, it can be concluded that at higher frequencies the adjacent portion of ground plane near the feed line becomes the dominating region in radiating field.

Figure 3.3 Evolution stages of basic UWB antenna

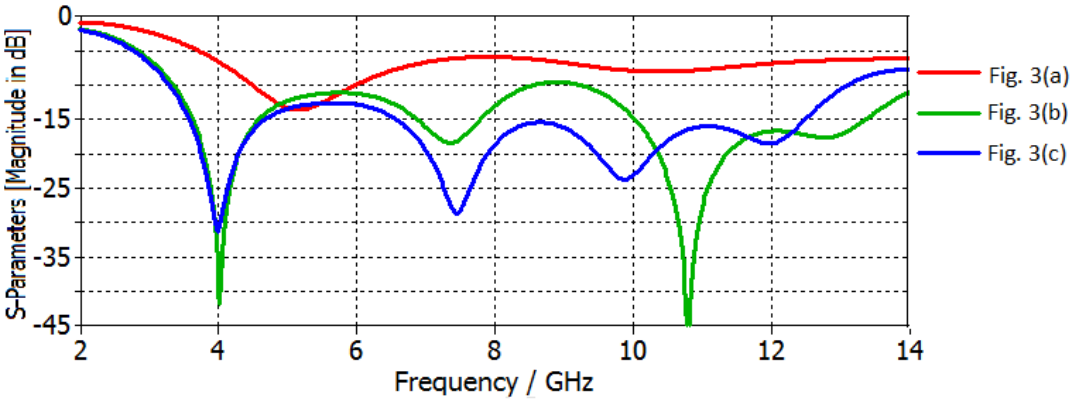

Figure 3.4 Return loss plot of evolution stages of basic UWB antenna

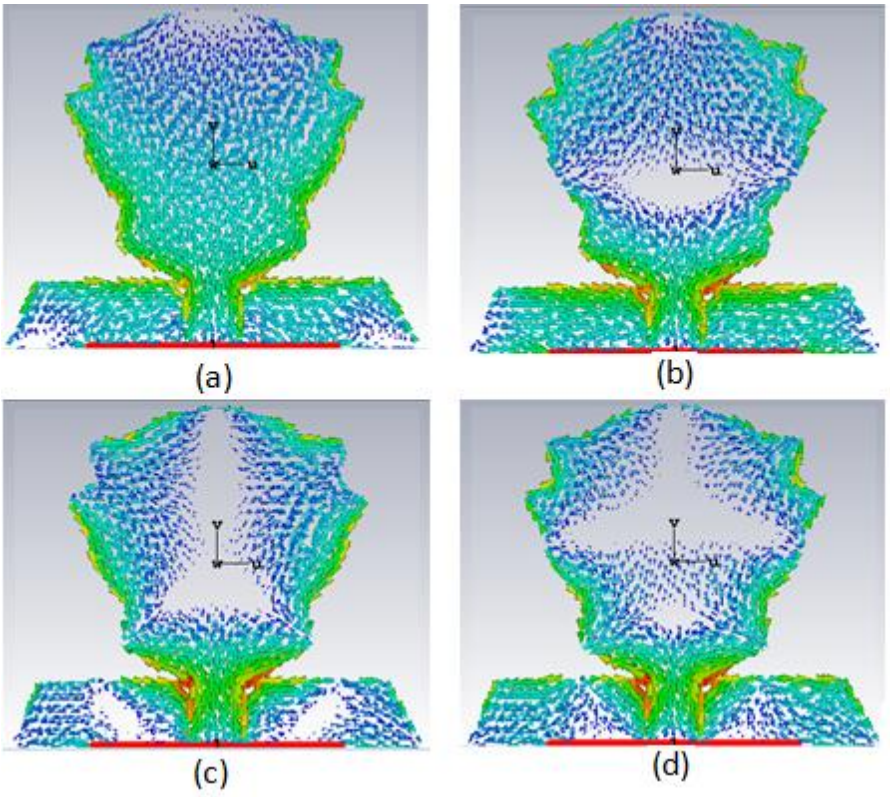

Figure 3.5 Surface current distribution of basic UWB antenna at four resonance frequencies (a) 4 GHz, (b) 7.5 GHz, (c) 9.9 GHz and (d) 12 GHz

3.3.2. Individual Band Notch Technique

Any undesired band can be strongly rejected, if the current distribution at that particular frequency band is confined in any part of the antenna. In this proposed antenna, five interfering bands have been rejected. These bands are WiMAX (3.3–3.7 GHz), aeronautical radio navigation (ARN) band (4.2–4.5 GHz), WLAN (5.15–5.85 GHz), ITU-8 band (7.9–8.5 GHz) and amature radio band (10–10.5 GHz). Different techniques have been used to reject these aforesaid bands. It can be observed from Figure 3.6 that surface current distribution is more at the outer boundary of the patch and it is negligible in the central portion of the radiating patch, feed line and ground. Therefore, band notching can be created by applying different types of slots in these non-radiating parts of the basic UWB antenna. All the dimensions of the antenna with the notching elements are tabulated in the Table 3.1.

Table 3.1 Parameter dimension (in mm)

Parameter	Size(mm)	Parameter	Size(mm)	Parameter	Size(mm)
h_s	1.6	R_a	1	T_5	0.3
h_p	0.035	R_{min}	8	T_g	0.4
L_s	24	R_{max}	9.3	W_n	7.2
L_p	13	R_1	7	W_p	13
L_g	4.5	R_2	4	W_s	29
L_n	1.5	R_3	1	W_1	2.6
L_b	2.5	T_1	0.5	W_2	1.4
L_1	2.5	T_2	0.7	Th_1	160°
L_2	3.5	T_3	0.4	Th_2	300°
L_3	2.3	T_4	0.3	Th_3	92°
G_i	0.4	G_a	0.3		

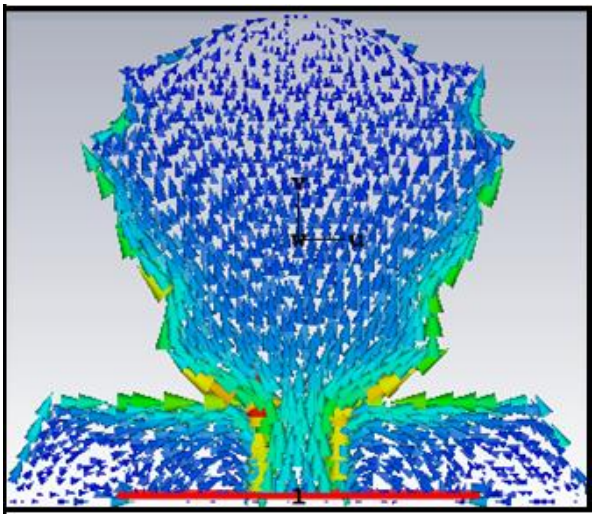

Figure 3.6 Surface current distribution of basic UWB antenna

3.3.2.1 WiMAX Rejection

Figure 3.7(a) exemplifies the antenna for WiMAX band rejection. Length of the slot is decided from the equation [20],

$$L_{n_i} = \frac{c}{2 \times f_{n_i} \times \sqrt{\varepsilon_{eff}}} \tag{3.3}$$

Where L_{n_i} is the length of slot for particular notching frequency $i = 1,2,3,4,5$.

An inverted arc shaped slot has been etched at the upper portion of the radiating patch. The inner radius and thickness of the arc are r_1 and t_1 respectively. The arc creates an angle $Th1$ at the

center and both the ends of the arc are extended vertically downwards to a length of L_1. Length of the arc is $A_1 = \frac{\left(\pi \times \left(R_1 + \left(\frac{T_1}{2}\right)\right) \times Th1\right)}{180}$. Total length of the slot, $L_{s_1} = A_1 + 2L_1$. Figure 3.8(a) clearly depicts the surface current distribution at 3.6 GHz is confined at the slot only and no radiation takes place outside the slot, furthermore direction of current at the at the two parallel edges are opposite to each other which strongly prevents any radiation except the particular notch.

3.3.2.2 ARN Band Rejection

Figure 3.7(b) exemplifies the antenna for ARN band rejection. To reject this band notching element is a split ring resonator (SRR). Dimension of the SRR has been decided according to the equation (3.1) and (3.2). The effective length of the arc according to the above said equation has been found as 20.98 mm. But the optimized length of the SRR is 22.76 mm. which has been calculated as; $A_2 = \frac{\left(\pi\left(r_2 + \left(\frac{t_2}{2}\right)\right) Th2\right)}{180}$. Inner radius and thickness of SRR are r_2 and t_2 respectively. Figure 3.8(b) clearly depicts the surface current distribution at the center frequency of this band is confined at the SRR only, and no radiation takes place outside the slot.

3.3.2.3. WLAN Rejection

Figure 3.7(c) exemplifies the antenna for WLAN rejection. Two symmetrical slits have been etched in the ground. This is a new technique applied in the CPW ground which is different from previous UWB antennas. In this case, length of each slit is, $L_g = \frac{\lambda_g}{4}$ *i.e.* quarter of the guided wavelength of the center frequency of this band. Therefore it can be concluded that the length of open ended notch element is quarter of the guided wavelength. The dimension of the slits can be calculated as $L_{s_2} = W_n + L_n$. Figure 3.8(c) clearly depicts the surface current distribution at the center frequency of this band is confined at the slits in the grounds only, and no radiation takes place outside the slits.

3.3.2.4. ITU-8 Band Rejection

Figure 3.7(d) shows the antenna for ITU-8 band rejection. Two concentric rectangular split ring resonators are etched from the feed. In this case, length of the resonator is of half of the guided wavelength of the center frequency of this band. The dimension of the resonator has been

calculated as$L_{s_4} = 2W_2 + 2L_2 - G_i$. Figure 3.8(d) clearly depicts the surface current distribution at 8.2 GHz which is confined within the two symmetrical rectangular SRRs and no radiation takes place outside these SRRs.

3.3.2.5. Amature Radio Band Rejection

Figure 3.7(e) exemplifies the antenna for WLAN rejection. Two symmetrical circular split ring resonators are etched from the lower portion of the patch. In this case, length of the resonator,$L_{s_5} = 2\pi R_a - G_a$. Figure 3.8(e) clearly depicts the surface current distribution at 10.2 GHz which is confined within the two symmetrical circular SRRs and no radiation takes place outside these SRRs. All the parameters are optimized by using the parameter sweep option in-built in CST MWS V14.0 to get best desired results. The individual dimensions of all the antenna design parameters and their notching elements are tabulated in Table 3.1. The aforementioned five individual notching elements are incorporated in the basic UWB antenna as shown in Figure 3.7(f). Figure 3.9 illustrates the effect of individual notches and all the five notches altogether on the performance of the basic UWB antenna. The comparative measurement of calculated and optimized length of each notching element is presented in Table 3.2. All the parameters are optimized to get best result. The dimensions of all the notching elements are listed in Table 3.1.

The aforementioned five individual notching elements are incorporated in the proposed notched UWB antenna as shown in Figure 3.1. Figure 3.9 illustrates the effect of individual notches and all the five notches altogether on the performance of the basic UWB antenna. The comparative measurement of calculated and optimized length of each notching element is represented in Table 3.2.

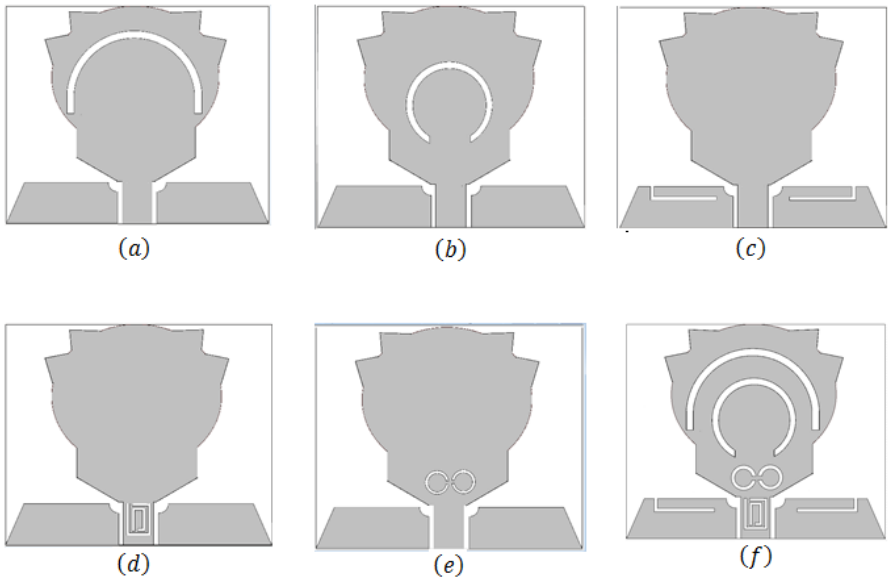

Figure 3.7 UWB antenna with individual band notching technique and final antenna with quintuple band notching technique

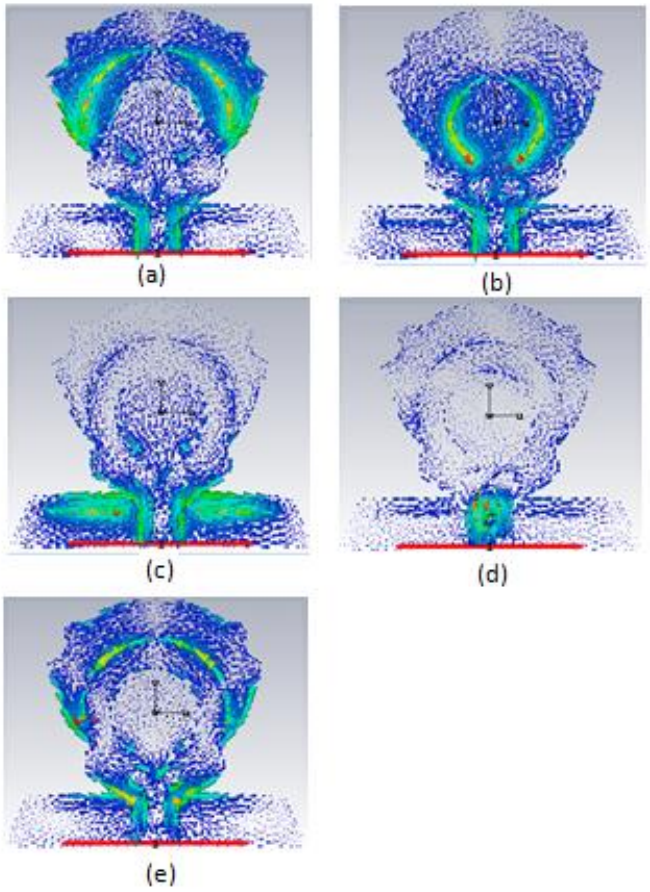

Figure 3.8 Surface current distribution of proposed quintuple notched UWB antenna at (a) 3.5 GHz, (b) 4.2 GHz, (c) 5.5 GHz, (d) 8.2GHz and (e) 10.2 GHz

Table 3.2 Comparison between the calculated, simulated and measured length of the five notching element

Parameters/band notch	WiMAX	ARN	WLAN	ITU-8	Amature radio band
Calculated slot length $\frac{\lambda_g}{2}$ (mm)	26.29	20.98	16.72	11.21	8.9
simulated slot length (mm)	25.24	22.75	8.7	10.7	6
Error between calculated and optimized slot length	-0.04	0.08	0.04	-0.05	-0.5

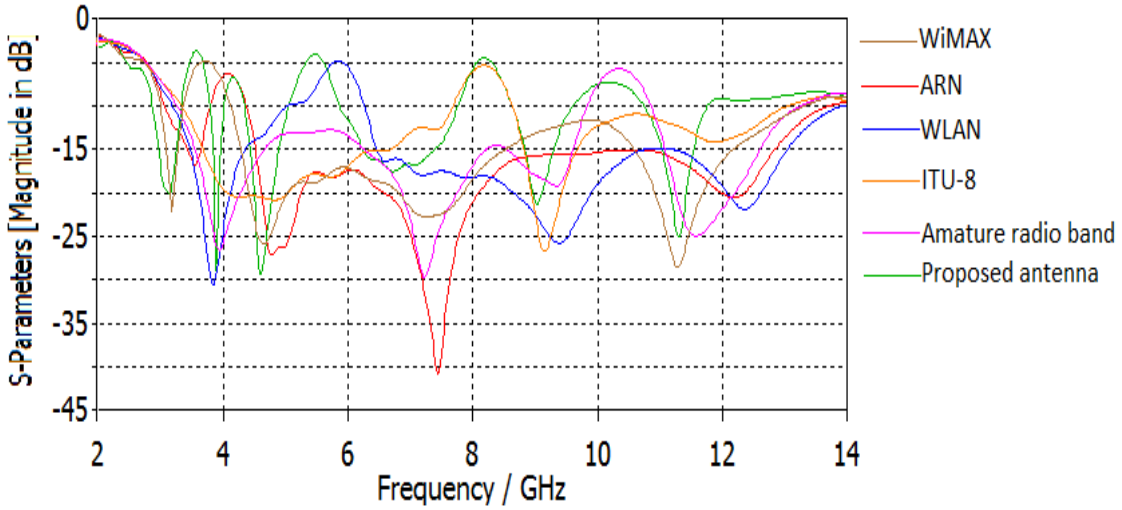

Figure 3.9 S_{11} Characteristic curve of each single band notched antenna and the proposed antenna

3.3.3 Parametric Study

To get a clear idea about the antenna performance, study of some of the antenna parameters has been performed. The calculated $\frac{\lambda_g}{2}$ (λ_g is the length of guided wavelength) length for WiMAX band is 26.082mm, whereas the optimized length of notching element for this band is observed as 25.24 mm. If the inner radius for this band i.e. R_1 is increased, then the stop band gradually shifts towards left side i.e. towards lower frequency as shown in Figure 3.10.

The calculated $\frac{\lambda_g}{2}$ length for ARN band is 20.98 mm, whereas the optimized length of notching element for this band is observed as 22.75 mm. If the angle of the split ring i.e. Th_2 is varied from 280° to 320°, then it has been observed that the stopband shifts towards right side for lower angle and towards left for higher angle. Best result has been observed for 300° angle, which is very clearly depicted in Figure 3.11.

The calculated $\frac{\lambda_g}{2}$ (λ_g is the length of guided wavelength) length for WLAN band is 16.72 mm, but the optimized length is 8.7mm *i.e.* near to$\frac{\lambda_g}{4}$. If the width of the corresponding slot for WLAN *i.e.* W_n is varied, it has been observed that the stop band shifts towards right for less width, which can be viewed in Figure 3.12.

The calculated $\frac{\lambda_g}{2}$ (λ_g is the length of guided wavelength) length for ITU-8 band is 11.21mm, but the optimized length is 10.7mm *i.e.* near to$\frac{\lambda_g}{4}$. If the slot gap of RSRR, G_i is varied, it has been observed that the width of the notch changes, as clearly depicted in Figure 3.13.

The calculated $\frac{\lambda_g}{2}$ (λ_g is the length of guided wavelength) length for Amature band is 8.9mm, but the optimized length is 6mm. If the radius of the corresponding slot for amature band *i.e.* R_a is varied, it has been observed that the stop band shifts towards right for smaller radius.

From the parametric study as depicted in Figure 3.10–3.14, it has been concluded that notching band shifts towards lower frequency for lesser length of the notching element. It is also observed that variation of any parameter of any particular notch band does not affect other bands. Best result can be achieved by adjusting the position and size of the notching element. The surface current distribution of the proposed antenna has also been studied for all the notching bands. The antenna surface current distribution has been shown in Figure 3.8(a–e), from where it can be concluded that the surface current at any particular notch frequency is confined in the corresponding notching element only and not in any other part of the antenna. The direction of current in each notching element is opposite and as a result any radiating field has not produced and at the same time stop band has been achieved. The comparison between the magnitude of reflection coefficient of simulated and measured bandwidth of notches and notch centre frequencies are listed in Table 3.3.

Table 3.3 Comparison between the five rejected notch frequency and their corresponding bandwidth

Characteristics/ band notch	WiMAX	ARN	WLAN	ITU-8	Amature radio band
Theoretical BW (GHz)	3.3–3.7	4.2–4.5	5.15–5.85	7.9–8.8	10–10.5
Simulated BW (GHz)	3.3–3.8	4.02–4.34	5.06–5.87	7.77–8.6	9.6–10.7
Measured BW (GHz)	3.45–3.95	4.1–5.05	5.35–6.25	7.6–8.6	9.45–10.5
Designed notch frequency (GHz)	3.5	4.35	5.5	8.2	10.25
Simulated notch frequency (GHz)	3.6	4.2	5.5	8.2	10.2
Measured notch frequency (GHz)	3.65	4.4	5.7	8.4	10.3

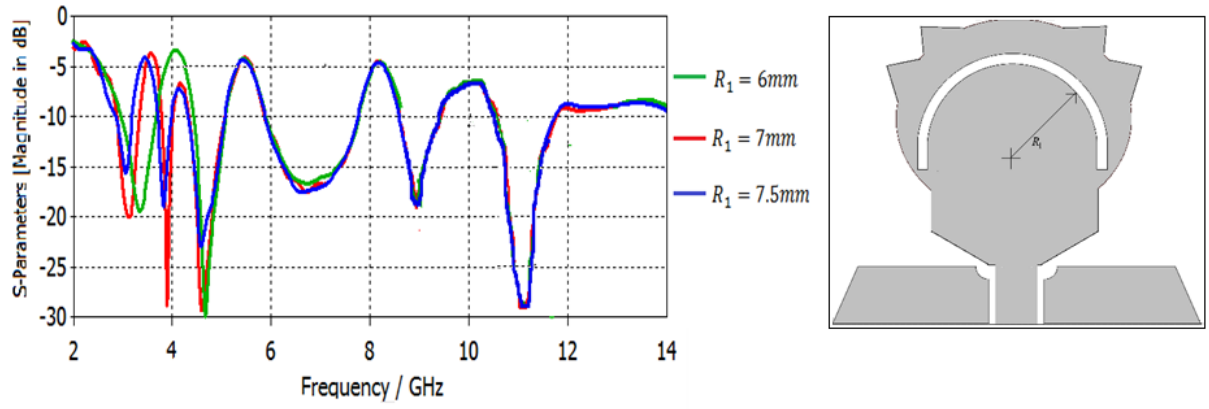

Figure 3.10 S11 magnitude of the proposed antenna as a result of the parametric variations of R_1 for rejecting WiMAX band

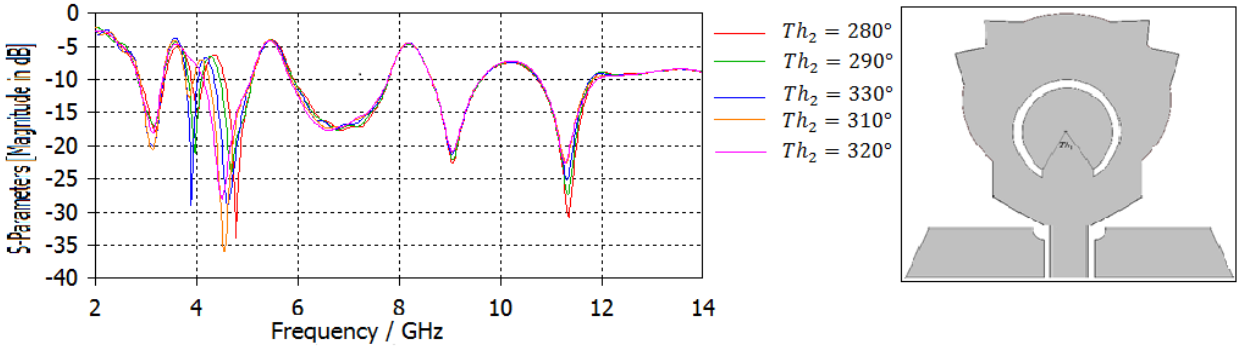

Figure 3.11 S11 magnitude of the proposed antenna as a result of the parametric variations of Th_2 for rejecting ARN band

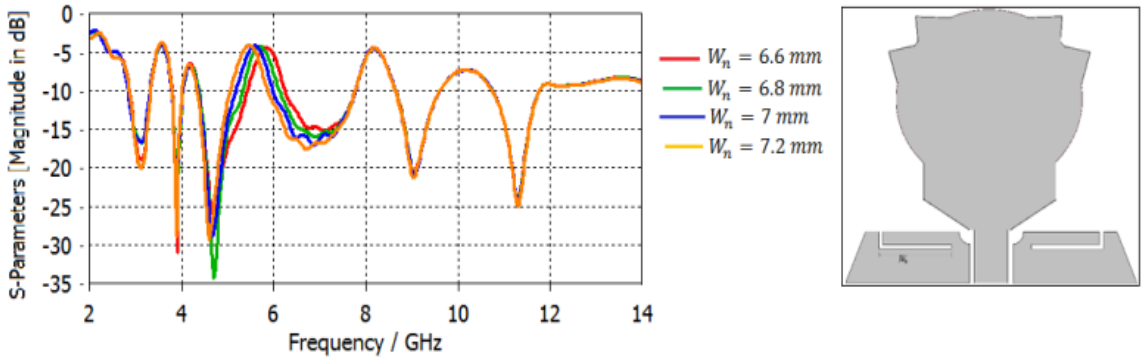

Figure 3.12 S11 magnitude of the proposed antenna as a result of the parametric variations of W_n for rejecting WLAN band

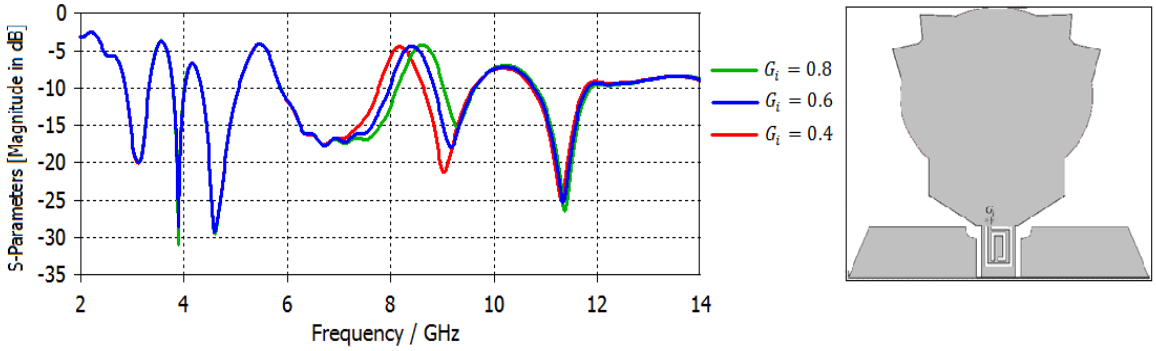

Figure 3.13 S11 magnitude of the proposed antenna as a result of the parametric variations of G_i for rejecting ITU-8 band

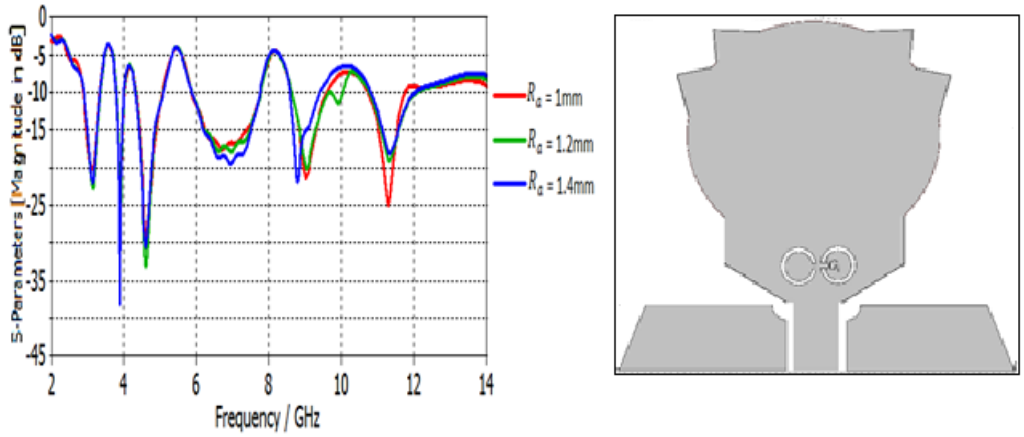

Figure 3.14 S11 magnitude of the proposed antenna as a result of the parametric variations of R_a for rejecting Amature radio band

3.3.4 Input Impedance and Equivalent Circuit Analysis

In order to study the rationale concerning the band notched slot elements, the input impedance characteristics of the proposed antenna are illustrated in Figure 3.15. It is very clearly depicted in the input impedance characteristics plot that the resistance at the resonance band is near about 50 Ω whereas the reactance at the same band is very close to zero. As discussed in [47], at both the notches the input impedance is high at the lower cut off frequency of the notch and at the same time reactance is altering from positive to negative which resembles a series RLC circuit, whereas at both the notches the input impedance is low at the higher cut off frequency of the notch and at the same time reactance is varying from negative to positive which resembles a parallel RLC circuit. As conferred in [48], at all the five notch frequencies the resistance is minimum and consequently the reactance is having positive slope which resemble to the characteristics of series resonant circuit. As stated in [49], the reactance curve reveals a series resonance characteristic and the resistance is close to zero at the lower notch frequency whereas at the higher notch frequency the reactance curve shows a parallel resonance characteristic and the resistance has a high value. The input impedance characteristics at the notched band are shown in elliptical region. The resistive values are very high as 85 and 191 Ω at the first and fourth notched frequencies respectively whereas the reactive values are negative at the same frequencies, which resemble the characteristics of RLC parallel resonant circuit (R_1, L_1, C_1 for first notch and R_4, L_4, C_4 for fourth notch), It can be observed that at the remaining notched frequencies, the resistive values are at minimum level and subsequently the reactive values are with positive slope which resemble to the characteristics of series resonant circuit (R_2, L_2, C_2 for second notch, R_3, L_3, C_3 for third notch and R_5, L_5, C_5 for fifth notch). By observing the input impedance characteristics, an approximated equivalent circuit of the proposed antenna is modelled in CST, which is shown in Figure 3.16. The equivalent circuit consisting RLC lumped element has been clearly depicted in Figure 3.17.

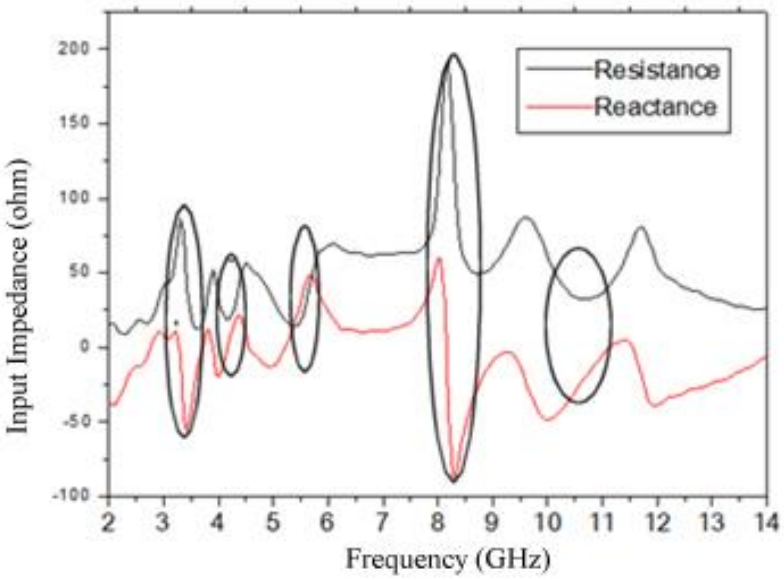

Figure 3.15 Input impedance characteristics of the proposed antenna

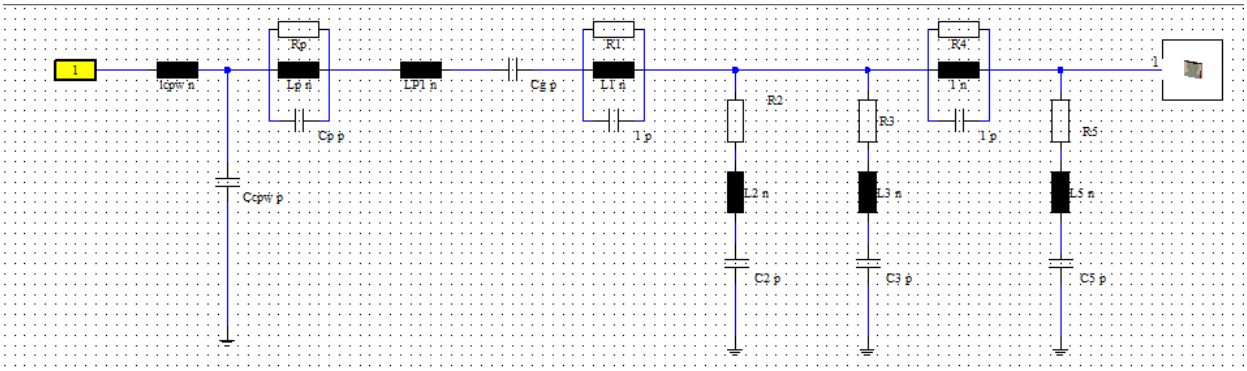

Figure 3.16 R-L-C resonant circuit model of the proposed antenna in CST Design Studio optimization setup

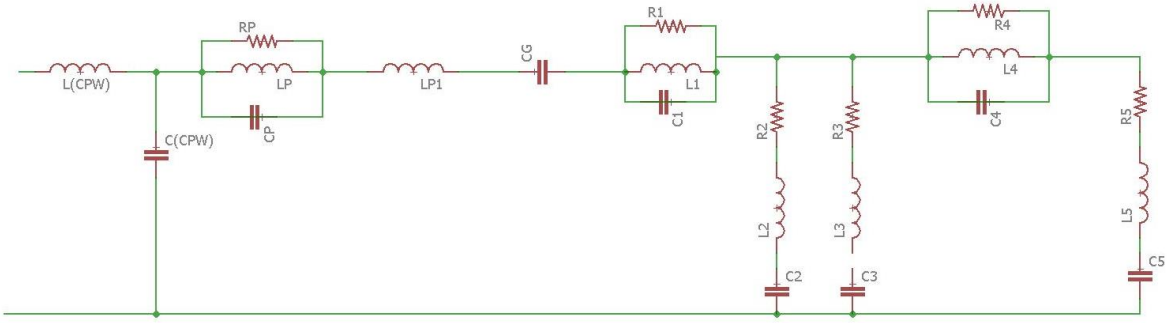

Figure 3.17 Equivalent RLC circuit of the proposed antenna

3.3.5 Gain and VSWR of Basic UWB and Proposed Antenna

The gain comparison of proposed antenna with basic UWB antenna has been clearly depicted in Figure 3.18. The gain of basic UWB antenna is in the range 1.23 dB–5.78 dB over 3.2–13.1 GHz, whereas the gain of proposed antenna is in the range -6.3–5.75 dB with noticeably reduced gain at the center frequencies of the notched bands. The gain values at WiMAX, ARN band, WLAN, ITU-8 and Amateur Radio bands are -6.2 dB, -4 dB, -4.65 dB, -2.12 dB and 3.03 dB respectively i.e. gains at the notched frequencies are reduced by 10 dB, 7.9 dB, 8.8 dB, 6.7 dB and 2.8 dB with respect to the basic UWB antenna due to the non-radiating behavior outside the notch.

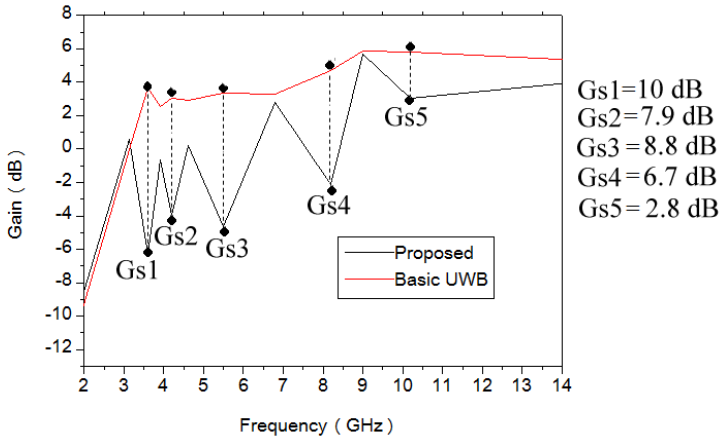

Figure 3.18 Comparison between the simulated gain of basic UWB antenna and proposed antenna (Gs_i= gain suppression for i^{th} band)

The performance of the proposed antenna can also be visualized in Figure 3.19, in which the VSWR magnitude of basic UWB antenna and proposed antenna with five band rejection features has been compared. For the basic UWB antenna, the magnitude of VSWR is less than 2 dB for the full band, whereas the magnitude of VSWR increases above 2 dB at the notch frequencies.

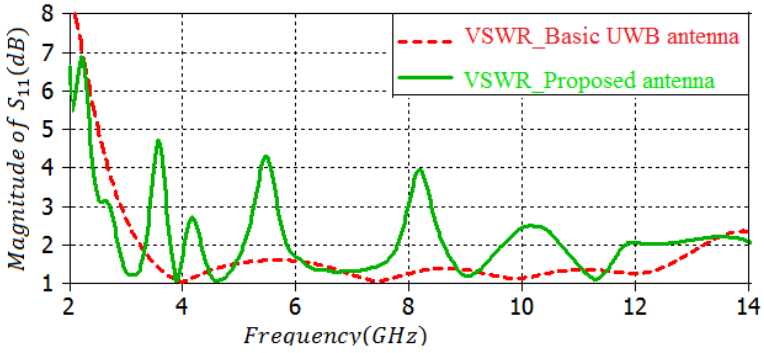

Figure 3.19 Comparison plot for VSWR of basic UWB antenna and quintuple notched proposed antenna

3.4 ANTENNA MEASUREMENT RESULTS AND DISCUSSIONS

The proposed split ring resonators based printed compact monopole UWB antenna with spiked elliptical radiator having five band rejection features is tested followed by fabrication as shown earlier in Figure 3.2. The return loss characteristics, VSWR and group delay of the proposed fabricated antenna has been tested and analyzed in Agilent E5071C vector network analyzer. The magnitude of S_{11} parameter of both the simulated and measured results of the proposed antenna is demonstrated in Figure 3.20. There are some divergences in the measured results from the simulated. The disagreement is associated to the fabrication error due to the skinny thickness of the copper printed on substrate. The SMA connector which has been soldered with the proposed miniaturized antenna for testing purpose also affects the performance of the antenna. An expert and commercial level fabrication of this prototype antenna will reduce errors significantly. The measured impedance bandwidth of the proposed antenna is 2.86–14 GHz having $|S_{11}| < -10$ dB level and five desired notches at 3.65, 4.4, 5.7, 8.4 and10.3 GHz. The result of comparative study regarding the notch bandwidth and notch center frequency of the proposed antenna has been listed in Table 3.3. Figure 3.21 demonstrates that there is a very good agreement between the simulated and measured results of VSWR (voltage standing wave ratio) of the proposed antenna. The measured result exhibits that the antenna has a wide bandwidth of 2.86–14 GHz having VSWR < 2 dB along with VSWR > 2 dB at the notches.

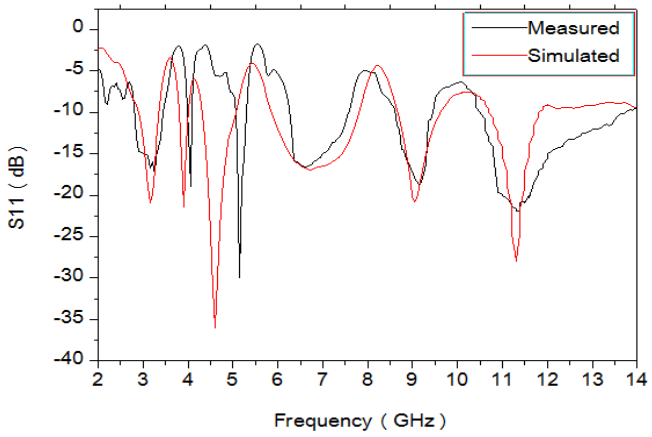

Figure 3.20 Simulated and measured S_{11} of the proposed antenna

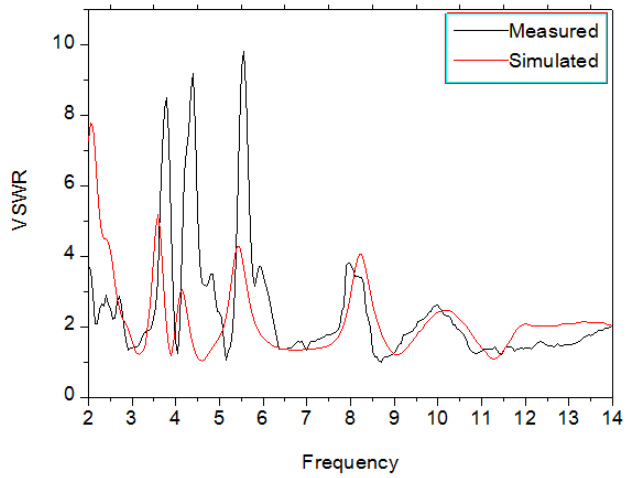

Figure 3.21 Simulated and measured VSWR curve for proposed antenna

The comparison between the measured and simulated gain has been picturized in Figure 3.22. There is a very good accordance between the two results.

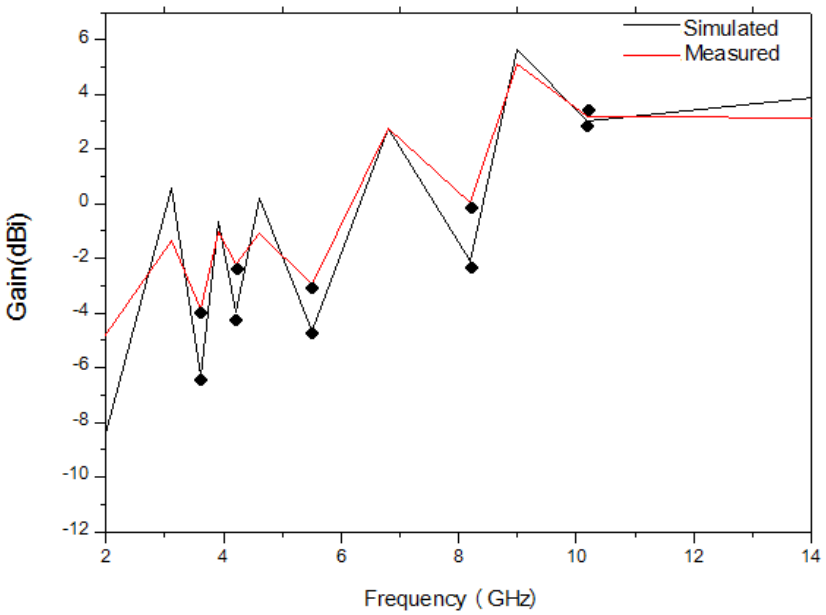

Figure 3.22 Simulated and measured gain of proposed UWB antenna

The measured radiation pattern of the proposed antenna in the far field has been executed in the Anechoic Chamber accessible at Millimeter Wave Laboratory, ECED in IIT, Roorkee. The measured radiation pattern has been clearly depicted in Figure 3.23(a–e). The proposed antenna has been imprinted in the *X*-*Y* plane, so *E* plane is represented by *Y*-*Z* plane and *H* plane is represented by *X*-*Z* plane.

E plane H plane

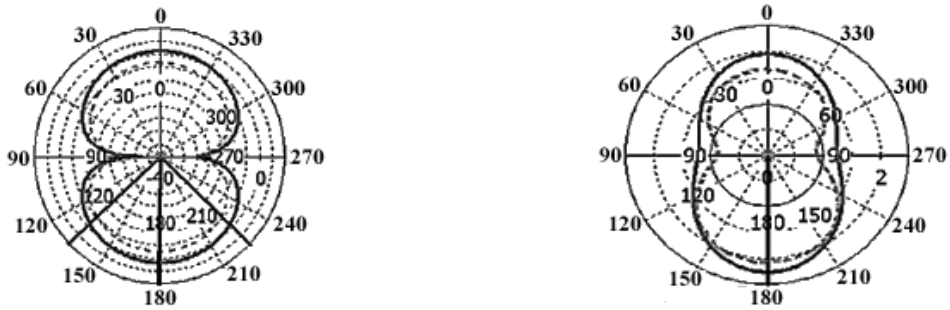

(a)

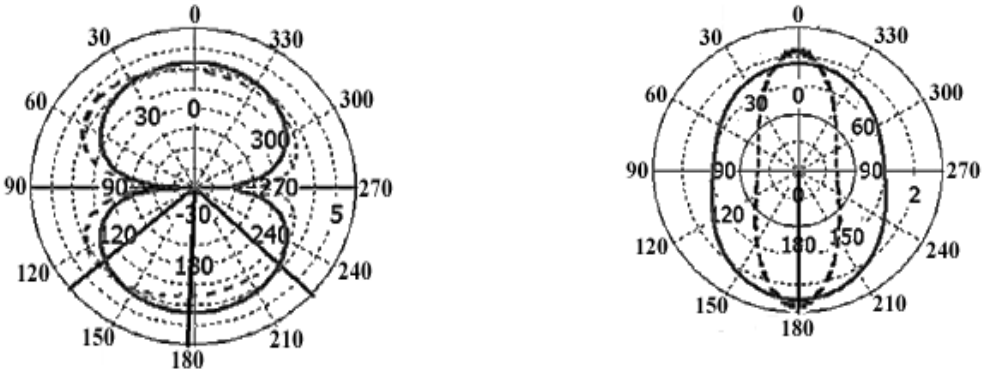

(b)

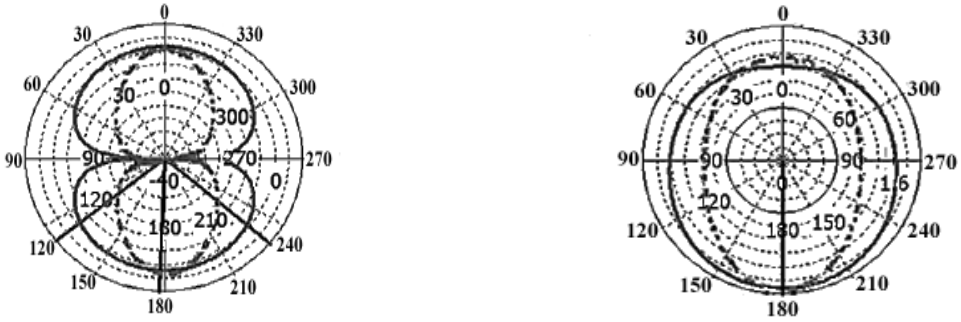

(c)

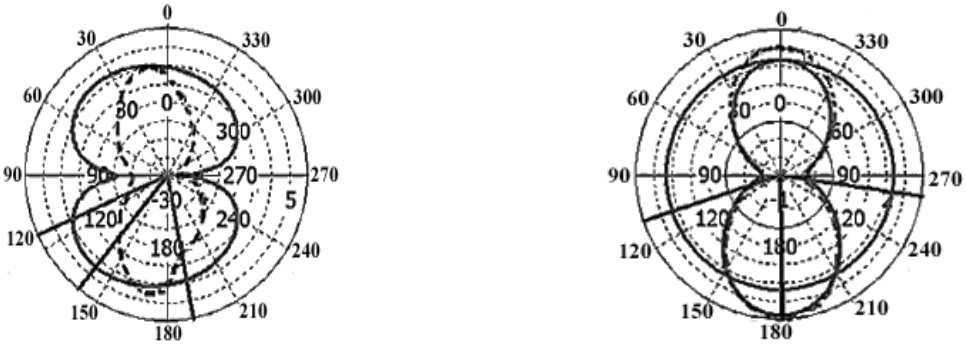

(d)

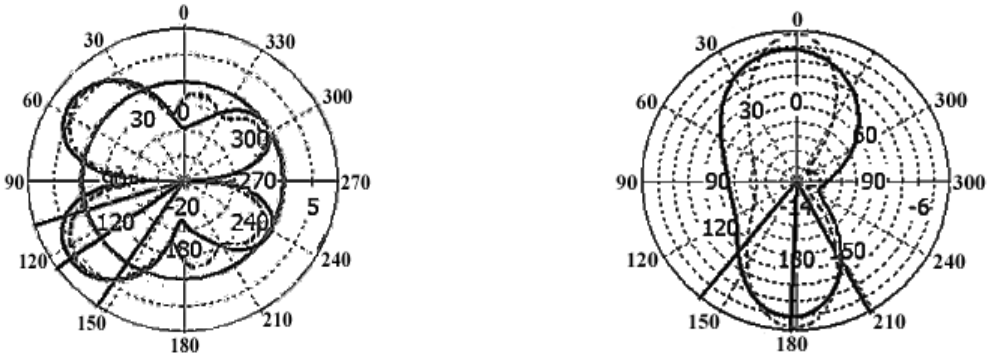

(e)

Figure 3.23(a–e) Measured Radiation pattern of the proposed antenna at (a) 3.12 GHz, (b) 3.9 GHz, (c) 4.6 GHz, (d) 6.8 GHz, (e) 9 GHz

The group delay measurement is one of the time domain performance parameters for UWB antenna. The response in the far-field region will be nonlinear, if the fluctuation in group delay variation exceeds 1 ns. If the group delay fluctuation exceeds 1ns, it will cause pulse distortion bands and as a result notch bands will be created.

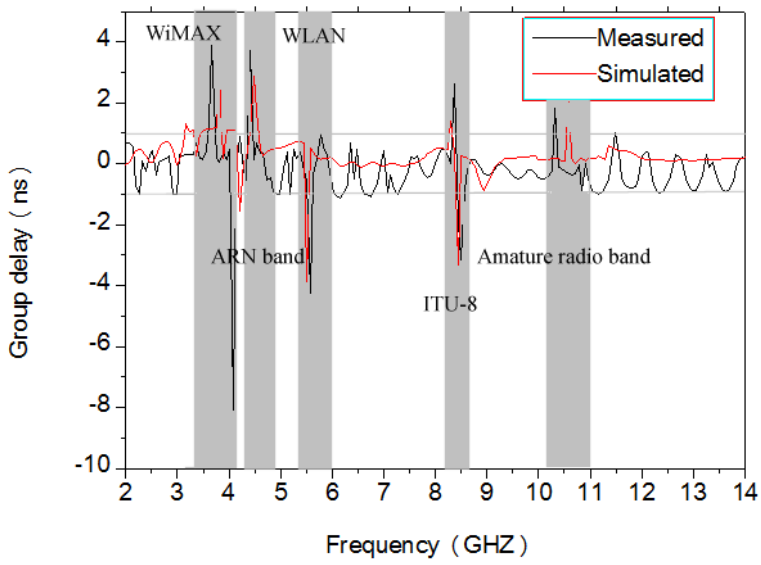

Figure 3.24 Simulated and measured group delay characteristics of fabricated proposed antenna

The simulated and measured group delay of the fabricated antenna is clearly depicted in Figure 3.24. The group delay fluctuation is between ± 1 ns for the resonant bands, but it exceeds the range in the notched bands. There are some discrepancies between the simulated and measured group delay which is caused by open air measurement. The group delay is more or less stable for the entire resonance band, but there is a sharp and huge change in the notches.

3.5 CONCLUSIONS

A compact monopole UWB antenna with five band notches has been proposed in this chapter. One extended arc and single SRR are used to get notches at WiMAX and ARN bands respectively. To get notch at WLAN, two symmetrical slots are etched in the CPW ground. For higher frequency notched *i.e.* for ITU-8 and amature band, two concentric rectangular SRR and two symmetrical single circular SRR are etched in the lowest portion of the patch and feed line respectively. The proposed antenna reveals good radiation properties in the resonance band and has a wider bandwidth. The basic UWB antenna has a moderate gain of 1.23 dB–5.78 dB. The gain at the notches is reduced as compared to the basic UWB antenna so the interference due to WiMAX, ARN band, WLAN, ITU-8 and Amature radio band can be successfully avoided.

CHAPTER 4

A COMPACT STEPPED MONOPOLE TRIPLE BAND-NOTCHED UWB ANTENNA WITH A COMPOSITE PARASITIC ELEMENT

4.1 INTRODUCTIO

In this chapter, a design of miniaturized triple-band notched monopole ultra-wide band antenna has been conferred. A broader bandwidth has been gained by using the stepped patch and appending adjacent triangles with the partial ground. Proper impedance matching has been achieved by appending a thin rectangle at the end of the feed line. A single composite parasitic element has been used to obtain triple band rejection. The proposed antenna is designed, fabricated and experimentally tested for the validation of results. The overall dimensions of the proposed antenna are $18\ \text{mm} \times 22\ \text{mm} \times 1.6\ \text{mm}$. The measured results show that the proposed antenna possesses three band notches centered at 4.5, 7.4 and 18.1 GHz to reject three bands e.g. 4–5 GHz, 7–8 GHz and 17.7–18.9 The sweep analysis of various notching elements is carried out to analyze the performance of antenna. The proposed antenna maintains omni-directional radiation pattern in H-Plane and dipole-like radiation pattern in E-plane. Further, stable gain over the whole UWB except at notched frequency bands is reported

4.2 ANTENNA DESIGN

The geometrical configuration of proposed UWB antenna with modified elliptical radiator with five band notched characteristics is shown in Figure 3.1. This antenna consists of two layers. The bottom layer is a substrate, made of dielectric material FR-4 (Flame Retardant-Fiber Glass Epoxy), the most popular inexpensive material to manufacture circuit boards, having relative permittivity (ε_r) 4.4, tangent loss (tan δ) 0.02 and thickness 1.6 mm. Both the patch and ground are made of PEC (Perfect Electric Conductor). The patch is printed on the top of the substrate and the partial ground is etched on the lower side of the substrate. The lower end of the feed line is appended by a rectangular extension for proper impedance matching. The proposed antenna has an overall dimension of $18 \times 22 \times 1.6\ \text{mm}^3$. The design simulation is carried out using three-dimensional electromagnetic simulation software Computer Simulation Technology Microwave Studio Version 2014 (CST MWS V14.0). The optimization of proposed antenna is carried out by using parameter sweep Eigen mode solver window. The basic UWB antenna

exhibits a simulated impedance bandwidth of 3.02 GHz–20.6 GHz. The feed line width has been designed to match characteristic impedance of 50 Ω using the following equations:

$$\varepsilon_{eff} = 0.5(\varepsilon_r + 1) + \frac{0.5(\varepsilon_r - 1)}{\sqrt{(1+\frac{12\square}{w_f})}} \quad (4.1)$$

$$Z_0 = \frac{120\pi}{\sqrt{\varepsilon_{eff}}[\frac{w_f}{\square}+1.39+0.67\ln(\frac{w_f}{\square}+1.44)]} \quad (4.2)$$

Where Z_0 is the characteristic impedance, ε_{eff} is effective permittivity of the substrate, w_f is feed line width and is □ substrate height.

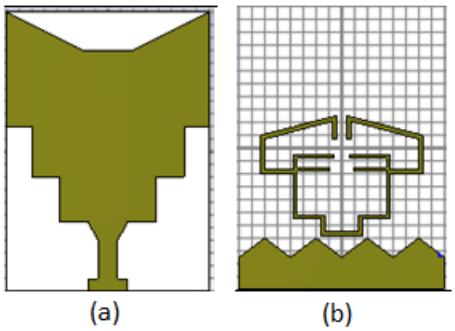

Figure 4.1 Top and bottom view of proposed UWB antenna with triple band-rejection features

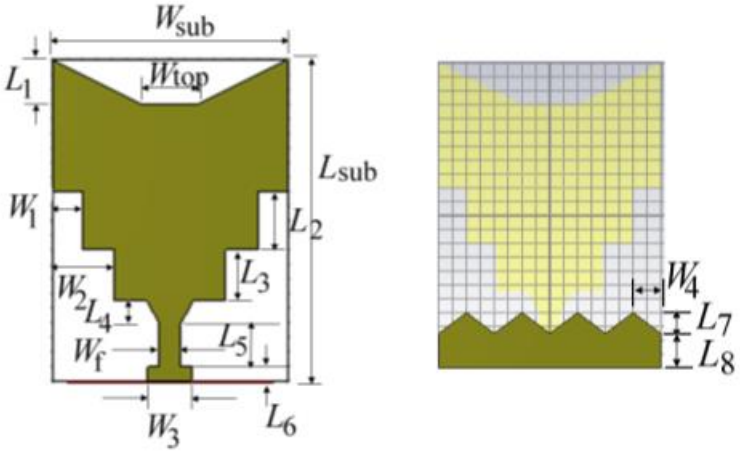

Figure 4.2 Dimension of basic UWB antenna

4.3 STEP-BY STEP APPROACH TO PROPOSED ANTENNA EVOLUTION

4.3.1 Basic UWB Antenna Design

Figure 4.3(a–d) shows step by step evolution of the basic UWB antenna. Initially the antenna had been designed as a rectangular patch incorporated with steps at the lower end and a partial ground as shown in Figure 4.3(a). But, this antenna exhibits only three resonating bands having

reflection coefficient< -10dB. The bands are 2.8–4.2 GHz, 5.65–8.6 GHz and 10.9–17 GHz as clearly depicted in Figure 4.4. This initial antenna is then modified and optimized to get a wide impedance bandwidth. In the first modification stage as shown in Figure 4.3(b), four adjacent triangles are appended with the partial ground and as a result an enhanced bandwidth has been achieved. In the next two stages of modification, a trapezoidal portion has been truncated and lower end of the feed line is appended with a rectangular extension to get wider bandwidth of 3–20.7 GHz and proper impedance matching of 50Ω. After the final modification, an impedance bandwidth of 3.2–13.1 covering the whole UWB range has been achieved with four resonance frequencies viz. 3.6 GHz, 7.2 GHz, 14.5 GHz and 18.7 GHz which is very clearly depicted in Figure 4.4.

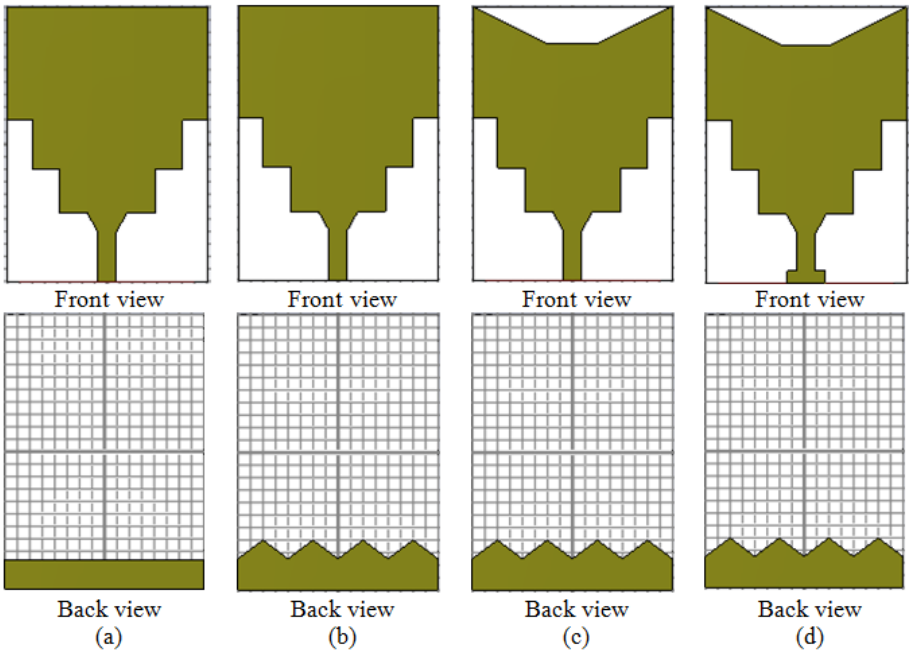

Figure 4.3 Evolution stages of basic UWB antenna

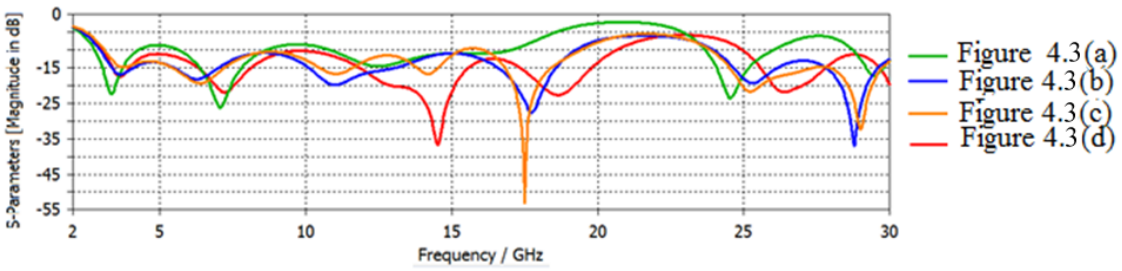

Figure 4.4 Return loss plot of evolution stages of basic UWB antenna

The VSWR characteristics of the basic UWB antenna have been clearly depicted in Figure 4.5. It can be inferred from the curve that the magnitude of VSWR remains below 2 dB for the whole UWB range.

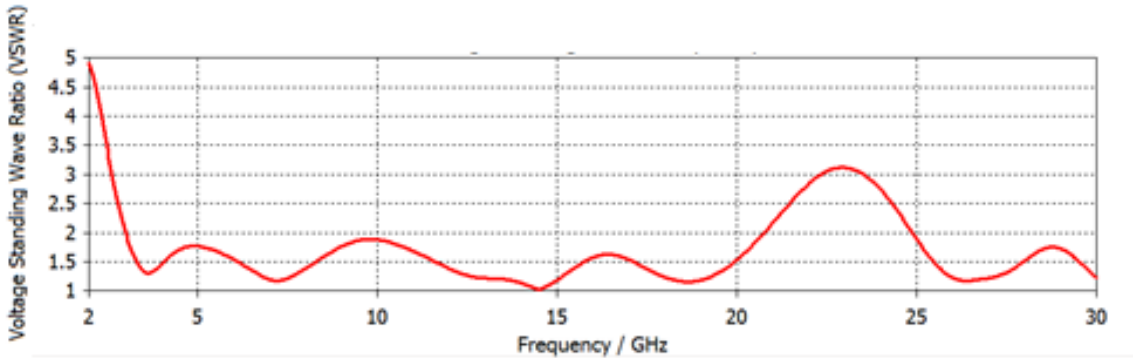

Figure 4.5 VSWR curve for basic UWB antenna

4.3.2. Individual Band Notch Technique

Any undesired band can be strongly rejected, if the current distribution at that particular frequency band is confined in any part of the antenna. In this proposed antenna, three interfering bands have been rejected. These bands are 4–5 GHz, 7–8 GHz, 17.7–18.9 GHz. A single composite parasitic element has been implanted to reject these aforesaid bands. All the dimensions of the antenna along with the notching elements are tabulated in the Table 4.1. The thickness of each parasitic element is 0.3 mm.

Table 4.1 Parameter dimension (in mm)

Parameter	Size(mm)	Parameter	Size(mm)	Parameter	Size(mm)
A_1	7.6	B_2	1.2	L_6	1
A_2	1.2	B_3	1.4	L_7	1.4
A_3	2.2	B_4	3	L_8	2.6
A_4	3.2	B_5	0.6	W_1	2
A_5	0.8	L_1	3	W_2	3.2
A_6	5.8	L_2	4	W_3	2.8
A_7	2.4	L_3	2.6	W_4	2
A_8	2	L_4	1.4	W_f	1.6
B_1	4	L_5	3		

4.3.2.1 First Band Rejection

Figure 4.6 exemplifies the notching element for first band rejection. Length of the slot is decided from the equation given below,

$$L_{n_i} = \frac{c}{2 \times f_{n_i} \times \sqrt{\varepsilon_{eff}}} \quad (3.3)$$

Where L_{n_i} is the length of slot for particular notching frequency $i = 1,2,3,4,5$ and c is the speed of light. Notching element corresponding to the first notching element is $\frac{\lambda_g}{2}$ resonator. The total physical length of the first parasitic element is $A_1 + 2B_1 + 2A_3 + 2B_2 + A_4 - A_2$=24.4mm. By implementing this notching element, a band of 4–5 GHz can be rejected. Therefore by implementing the first parasitic element the following frequency bands allocated for Aeronautical radio navigation, fixed mobile and fixed satellite mobile can be rejected.

4.3.2.2 Second Band Rejection

Figure 4.7 exemplifies the antenna for second band rejection. Two symmetrical strips are appended with the first parasitic element to reject this second lower frequency band. The physical length of the second notching element is $A_4 + 2B_2 + 2A_3 + 2A_6 + 2B_4 - A_2$=32 mm. This notching element is also $\frac{\lambda_g}{2}$ resonator. By implementing this notching element, a band of 6.9–7.9 GHz can be rejected. Therefore by implementing the second parasitic element the following frequency bands allocated for Meteorological satellite, Maritime mobile-satellite fixed mobile and fixed satellite mobile can be rejected.

4.3.2.3. Third Band Rejection

Figure 4.8 exemplifies the antenna for three band rejection. Two symmetrical I-shaped slits have been added to the previous parasitic element. The physical length of the third notching element is $A_4 + 2B_2 + 2A_3 + 2A_6 + 2A_7 + 2B_1 - 2B_5$=21.6 mm. The length of this resonator is λ_g. By implementing this notching element, a band of 17.5–18.9 GHz can be rejected. Therefore by implementing the third parasitic element the following frequency bands allocated for broadcasting satellite and earth-exploration satellite can be rejected.

All the parameters are optimized to get best result. The dimensions of all the notching elements are listed in Table 4.1. The aforementioned three individual notching elements are incorporated in the proposed notched UWB antenna as shown in Figure 4.2. The surface current distribution, picturized in Figure 4.9 can revealed that there is no radiation in the region out of the notching element at each notch center frequency. Because, the direction of current is opposite to each other at the two parallel edges and as a result the resultant current becomes nil and hence no radiation takes place. Figure 4.10 and Figure 4.11 illustrate the effect of individual

notches and the change in performance of the basic UWB antenna due to implementation of three notching elements.

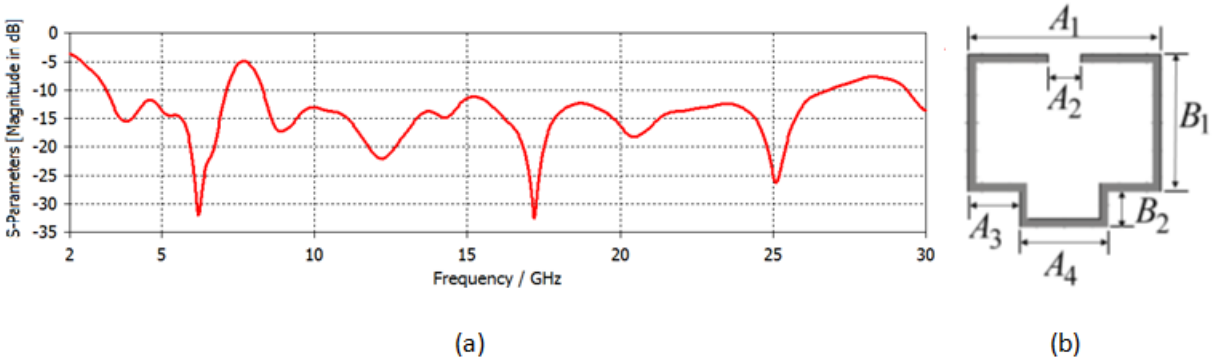

(a) (b)

Figure 4.6 UWB antenna with first notching element. (a) Simulated Return loss and (b) corresponding notching element

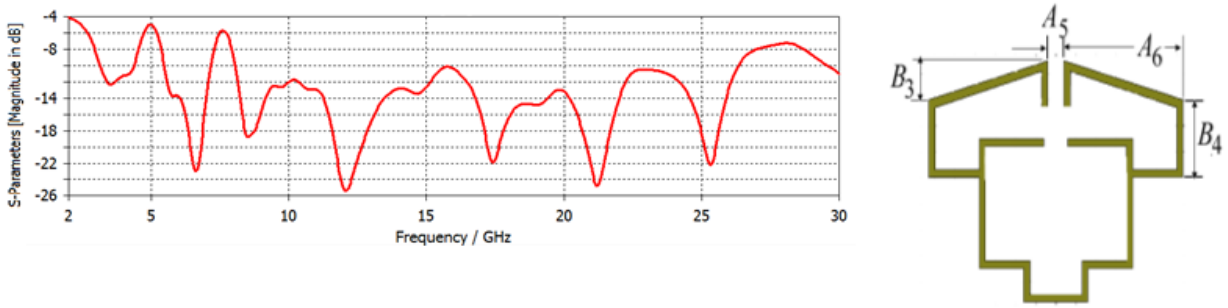

(a) (b)

Figure 4.7 UWB antenna with second notching element. (a) Simulated Return loss and (b) corresponding notching element

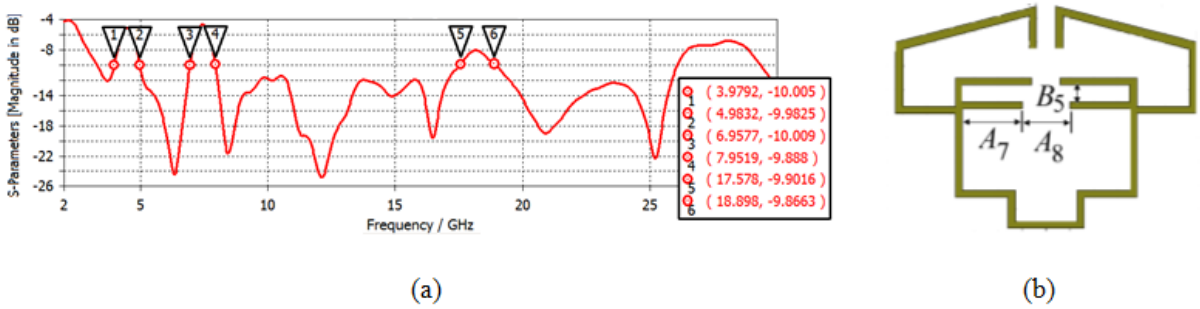

(a) (b)

Figure 4.8 UWB antenna with third notching element. (a) Simulated Return loss and (b) corresponding notching element

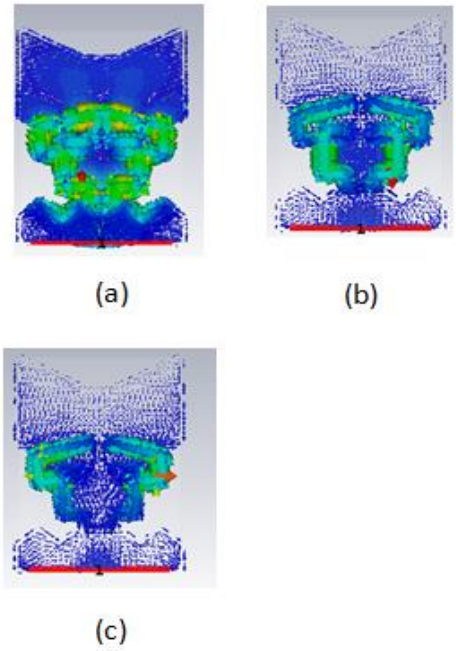

Figure 4.9 Surface current distribution of proposed quintuple notched UWB antenna at (a) 4.5 GHz, (b) 7.5 GHz and (c) 18.2 GHz

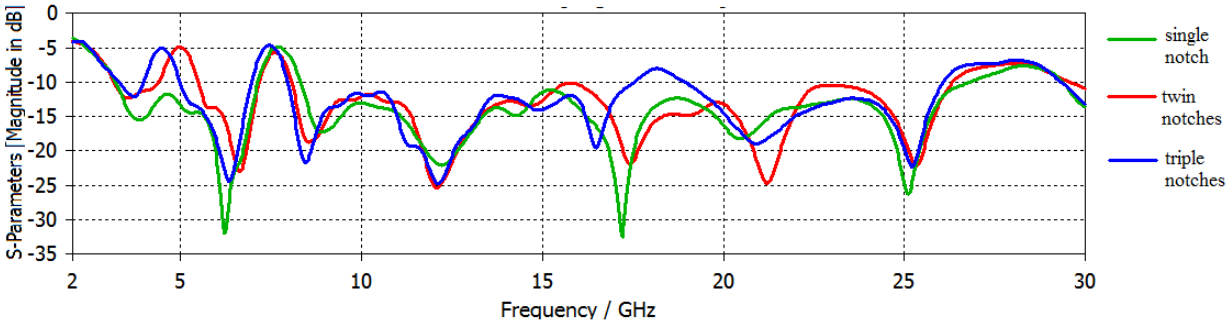

Figure 4.10 S_{11} Characteristic curve of step by step band notching effect

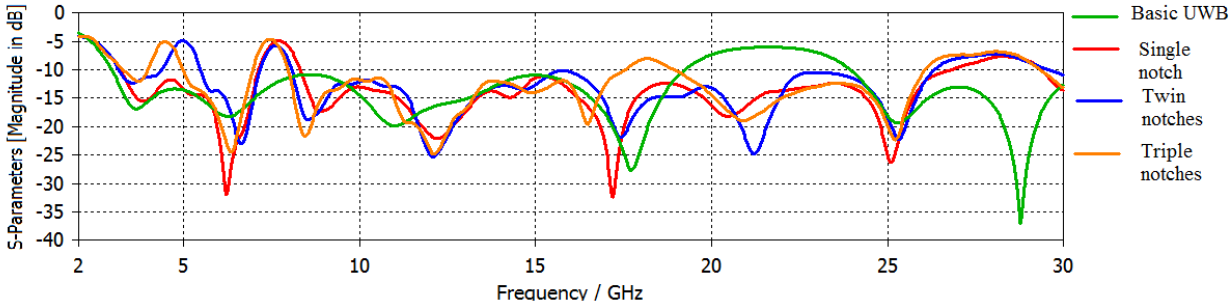

Figure 4.11 S_{11} Characteristic curve of step by step band notching effect along with the basic UWB antenna

4.4 SIMULATION RESULTS OF RETURN LOSS, VSWR AND RADIATION PATTERN OF PROPOSED ANTENNA

The return loss of the proposed antenna has been clearly depicted in Figure 4.12, from where it can be inferred that the magnitude of return loss is below 10 dB for resonance frequencies and above 10 dB at the notched frequencies.

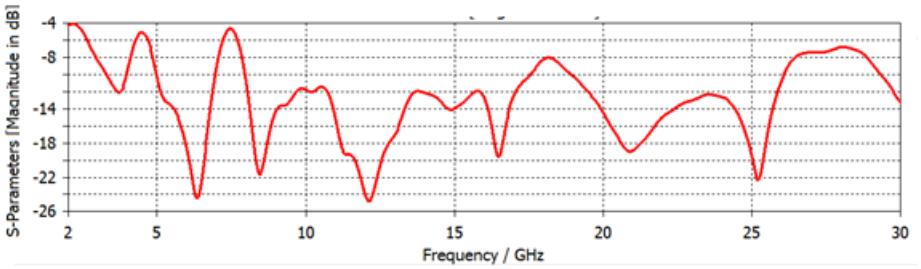

Figure 4.12 Return loss characteristic curve of the proposed antenna

The VSWR characteristics of the proposed antenna has been clearly depicted in Figure 4.13, from where it can be inferred that the magnitude of VSWR is below 2 dB for resonance frequencies and above 2 dB at the notched frequencies.

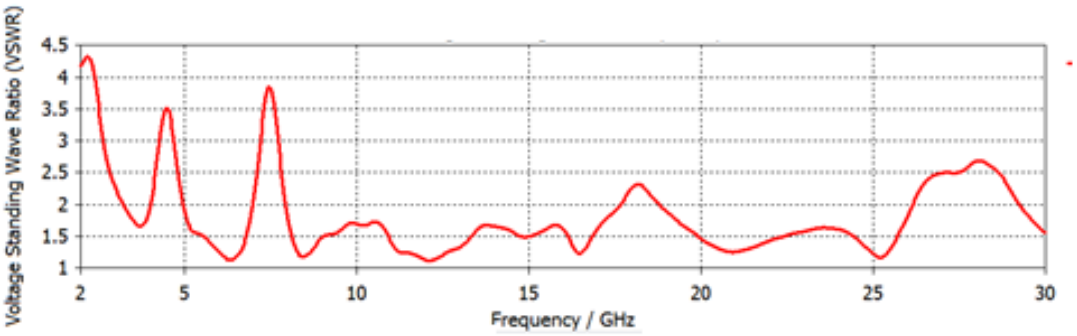

Figure 4.13 VSWR curve of the proposed antenna

Simulated radiation pattern of the proposed antenna has been shown in Figure 4.14. The proposed antenna has been imprinted in the *X*-*Y* plane, so *E* plane is represented by *Y*-*Z* plane and *H* plane is represented by *X*-*Z* plane.

H-plane E-plane

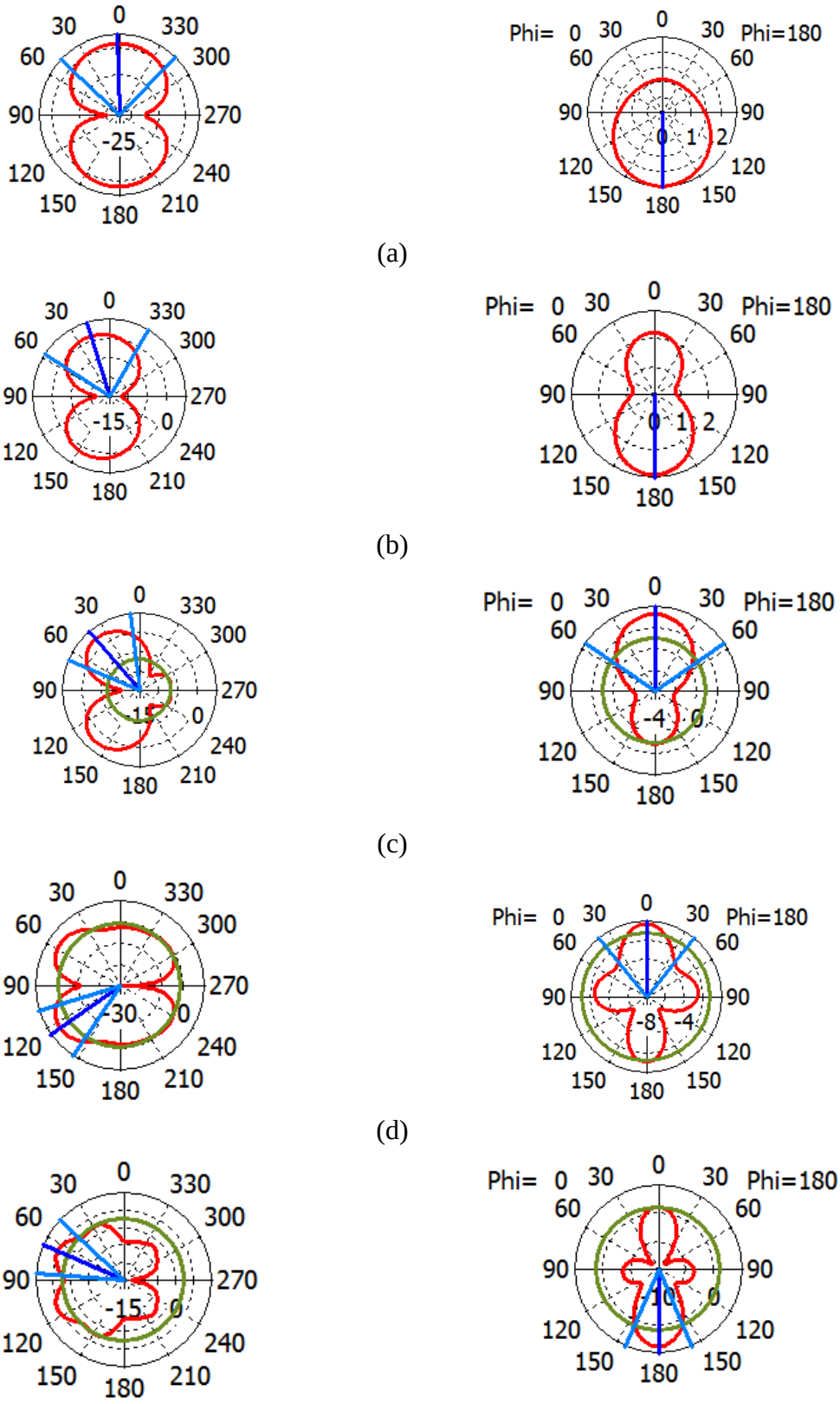

(a)

(b)

(c)

(d)

(e)

Figure 4.14 Simulated radiation pattern of the proposed antenna

4.5 CONCLUSIONS

In this chapter, a single composite structured parasitic element loaded triple band notched UWB antenna has been discussed. The patch is made stepped shaped at the lower end and the partial ground has been modified to achieve an enhanced bandwidth. A single composite parasitic element has been implanted at the bottom of the dielectric substrate.

CHAPTER 5

CONCLUSIONS AND SCOPE OF FUTURE WORKS

5.1 CONCLUSIONS

The research work sketched in this thesis was motivated by the increasing requirement for miniaturized, inexpensive UWB antenna possessing band rejecting capability; notched UWB antenna comes into existence to assist the rapidly flourishing market of ultra-wide band communication. The explore and advancement in modern have been concentrated on evolving and refining the electrical characteristics of microstrip antenna, enhancing the bandwidth, rejecting undesired bands and result of different feeding technique. In this thesis, CST microwave studio version 14 has been employed for the simulation purpose. CST microwave studio is based on Finite Integral Technique that agreements with integral equations in place of differential equations and this technique is based on a small scale explanation of Maxwell's equation.

The subsequent task was to survey various research papers related to notched UWB antenna design and development. It is not an easy task to design a compact antenna which has a broader bandwidth and at the same time undesired band rejection proficiency.

Due to the advancing requirement in a short time span, the UWB antenna with multiple band rejection proficiency fetched more interest. Looking at the enhancing demand of notched UWB antenna, this research work is aimed with design and development of such a compact antenna.

The following movement of this research work was to search some novel design of UWB antenna that can achieve the entire essential requirements microstrip antenna such as perfect impedance matching, enhanced wider bandwidth, better reflection coefficient, optimized gain, appropriate group delay *etc*. The elaborate contributions of this thesis are as follows:

Chapter 1 describes a brief introduction of microstrip antenna and UWB antenna. The reason behind the motivation towards notched UWB antenna has been portrayed in this chapter. The problem statement, research objective, scope and methodology have been depicted also.

Chapter 2 furnishes the MSA in detail, different feeding techniques, and methods of analysis, UWB antenna, and different notching techniques. Few literatures applying different notching techniques are also discussed in this chapter. Some research papers based on basic

UWB antenna and UWB antenna which applying various notching techniques are briefly discussed in this chapter.

Chapter 3 provides a compact CPW fed UWB antenna that has a measured bandwidth of 2.87–14 GHz. The basic UWB antenna provides a gain ranging 1.23–5.78 dB. In the basic UWB antenna has been implanted with two arc shaped slots in the radiating patch to reject WiMAX and ARN band. Two symmetrical slits are implanted in the CPW ground to get a stop band for WLAN. Rectangular and circular SRRs are incorporated in the feed line and lower part of the patch to get rejection at ITU-8 and amature radio band, respectively. All the simulated results are studied and analyzed. The antenna has been fabricated and tested also. The simulated results are compared with the measured one. The simulated group delay is in the range of ± 1 ns, which is in the acceptable range.

Chapter 4 provides a miniaturized parasitic element fed UWB antenna possessing a simulated bandwidth of 3.2–26.14 GHz. The patch is stepped and truncated at the top to get UWB band. A complicated single structured parasitic element has been implanted on the bottom of the substrate to get triple band rejection at 4–5 GHz, 6.9–7.9 GHz and 17.6–18.9 GHz bands.
Chapter 5 summarizes all the previous chapters and discussed about the future scope.

In conclusions, this thesis has fulfilled the aim of multiple notched monopole UWB microstrip patch antenna characterized with broader impedance bandwidth, raised gain at resonating bands at the same time minimum gain at the rejected bands, considerable reflection coefficient characteristics and in range group delay.

5.2 FUTURE SCOPE

- The feed line can be modified in different way to achieve best optimization
- More miniaturized UWB antenna can be designed to achieve desired band rejection
- Other feeding techniques such as coaxial feeding, aperture coupling, proximity coupling can be implemented

REFERENCES

[1] Jain K and Gupta K (2012). Different Substrates Use in Microstrip Patch Antenna-A Survey, *International Journal of Science and Research (IJSR),* 3(5), 2319-7064.

[2] Ma TG and Jeng SK (2005). A Printed Dipole antenna with tapered slot feed for ultra-wide band applications, *IEEE Tansactions on Antennas and Propagation*, 53(11), 3833–3836.

[3] Behdad N and Sarabandi K (2005). A Compact Antenna for ultra-wide band applications, *IEEE Tansactions on Antennas and Propagation*, 53(7), 2185–2192.

[4] Lodge, Electric telegraphy. U.S. Patent 609,154 (August 16, 1898).

[5] Wang W, Zhong SS and Liang XL (2004). A broadband CPW-fed arrow-like printed antenna, *IEEE Antennas and Propagation International Symposium (Digest),* Monterey, CA, Jul. 2004.

[6] Choi SH et al (2004). A new ultra-wideband antenna for UWB applications. Microwave and Optical Technology Letters 40(5), 399–401.

[7]Liang JX et al (2005) Study of a printed circular disc monopole antenna for UWB systems. IEEE Transactions on Antennas and Propagation, 53(11), 3500–3504.

[8] Ooi BL et al (2005). Wideband LTCC CPW-fed two layered monopole antenna. IEE Electronics Letters, 41(16), 889–890.

[9] Lizzi L et al (2010). Printed UWB antenna operating for multiple mobile wireless standars, *IEEE Antennas and Wireless Propagation Letters*, 10, 1429–1432.

[10] Balanis CA. *Antenna Theory: analysis and design*. John Wiley & Sons, 2016.

[11] James JR and Hall PS. *Handbook of microstrip Antennas*, IEEE Electromagnetic Waves Series 28, London, United Kingdom, Peter Peregrinus Ltd, 1989.

[12] Kumar G and Ray KP. *Broadband Microstrip Antennas*, Artech House, Boston, London, 2003.

[13]Deschamps GA. Microstrip Microwave Antennas, presented at the third USAF Symposium on Antennas, 1953.

[14] Gutton H and Baissinot G (1955). Flat Aerial for Ultra High Frequencies, French Patent No. 703 113 1955.

[15] Pozar DM. *Microstrip Antennas*. Proc. IEEE, 1992.

[16] Huang Y and Boyle K. *Antennas From Theory to Practice*, John Wiley & Sons Ltd, 2008.

[17]Newman EH and Tulyathan P (1981). Analysis of Microstrip Antennas Using Moment Methods *IEEE Transactions on Antennas And Propagation,* 29(1).

[18] Harrington RF et al (1992). Formulation of Boundary Integral Equations by the Equivalent Source Method (eds.), Boundary Element Technology, *Computational Mechanics Publications*.

[19] Federal Communication Commission, "First Report and Order, Revision of Part15 of the Commission's Rules Regarding Ultra-Wideband TransmissionSystem," FCC 02 48, 2002.

[20] Oppermann M, Hamalainen and Iinatti J, UWB Theory and Applications, *John Wiley & Sons, Ltd,* 2004.

[21] Jin Y, Tak J and Choi J (2016). Quadruple Band-Notched Trapezoid UWB Antenna with Reduced Gains in Notch Bands, Journal of Electromagnetic Engineering and Science, 16 (1), 35-43.

[22] Liu JJ, Esselle KP and Zhong SS (2013). Planar ultra-wideband antenna with five notched stop bands. Electron. Lett., 49 (9) (2013), 579-580.

[23] Mewara, H.S.; Jhanwar, D.; Sharma, M.M.; Deegwal, J.K.: A printed monopole eiipzoidal UWB antenna with four band rejections. Int. J. Electron. Commun (AEÜ)., 83 (2018), 222-232.

[24] Mewara, H.S.; Deegwal, J.K.; Sharma, M.M.: A slot resonators based quintuple band-notched Y-shaped planar monopole ultra-wideband antenna. Int. J. Electron. Commun (AEÜ)., 83 (2018), 470-478.

[25] Computer Simulation Technology — CST (Microwave Studio MWS), Version-2014.

[26] Balanis, C.A.: Antenna theory analysis and design, Wiley, 2005.

[27] Kim JP et al (2005). Design of an ultra wide-band printed monopole antenna using FDTD and genetic algorithm. *IEEE Microwave and Wireless Components Letters*, 15(6) 395–397.

[28] Low ZN, Cheong JH and Law CL (2005). Low-cost PCB antenna for UWB applications. *IEEE Antennas and Wireless Propagation Letters*, 4, 237–239.

[29] Osama A and Sebak AR (2008). A printed monopole antenna with two steps and a circular slot for UWB applications, *IEEE Antennas and Wireless Propagation Letters,* 7, 411–413.

[30] Alsaif H and Islam NE (2014). New Planar CPW Fed Antenna for UWB Applications with Excellent Performance, *International Journal of Innovative Research in Computer and Communication Engineering,* 2(11).

[31] Pandey GK et al (2014). Metamaterial Based Compact Antenna Design for UWB Applications DOI: 978-1-4799-2027-3/14

[32] Yadav A, Sethi D and Khanna RK (2016), Slot loaded UWB antenna: Dual band notched characteristics, International Journal of Electronic and Communication (AEÜ), 70, 331–335

[33] Yazdi M and Komjani N (2013). Planar Uwb Monopole Antenna with Dual Band-Notched Characteristics for UWB Applications, *Microwave and Optical Technology Letters* , 55(2).

[34] Abbosh A and Bialkowski M (2008). Design of UWB Antenna with Parasitic Elements for Multiband Rejection, DOI: 978-1-4244-2642-3/08.

[35] Kumar A and Sharma MM (2014). An extremely wide band printed antenna with WLAN stop band using SRR, *International Conf. on Signal Propagation and Computer Technology. (ICSPCT)*, [Ajmer, India, 12-13 July 2014].

[36] Islam MM et al (2014). A compact 5.5 GHz band-rejected UWB antenna using complementary split ring resonators, *Science World Journal*, 1-9. Article ID 528489.

[37] Saraswat RK et al (2017). Triple band-notch UWB antenna with SRRs and CSRRs. *International Journal of Latest Trends in Engineering and Technology,* 8 (2), 128–134.

[38] Yadav A, Sethi D and Khanna RK (2016). Slot loaded UWB antenna: Dual band notched characteristics. *International Journal of Electronic Communication (AEÜ),* 70, 331–335.

[39] Bhattacharya A et al (2017). Compact slotted UWB monopole antenna with tuneable band-notch characteristics, *Microwave and Optical Technology Letters,* 54, 2358–2365.

[40] Liao XJ et al (2011). Aperture UWB antenna with triple band-notched characteristics *Electronic Letters,* 47 (2), 77–79.

[41] Wang Z, XLiu J and Yin Y (2016). Triple band-notched UWB antenna using novel asymmetrical resonators, *International Journal of Electronic Communication (AEÜ),* 70 ,1630–1636.

[42] Vendik IB et al (2017). Ultra-wide band (UWB) planar antenna with single-,dual- and triple-band notched characteristic based on electric ring resonator, *IEEE Antennas and Wireless Propagation Leters,* 16, 1536–1225.

[43] Rehman SU and Alkanhal M (2017). Design and system characterization of ultra-wideband antennas with Multiple Band-Rejections, *IEEE Access*, 5 , 2169–3536.

[44] Sharma MM et al (2014). Compact planar monopole UWB antenna with quadruple band-notched characteristics, *Progress in Electromagnetic Research C,* 47, 29–36.

[45] Li T et al (2012). A compact ultra-wideband antenna with four band-notched – characteristics, *Microwave and Optical Technology Letters*, 54 , 2862–2865.

[46] Kaur A and Srivastava G (2016). CPW-Fed UWB Antenna with Multiple Band-Notches for WiMAX, WLAN and X-Band Satellite Downlink Communication Systems, *Interntional conference on Wireless Networks and Embedded Systems (WECON),* [Rajpura, India].

[47] Pandey GM et al (2016). Design and Analysis of Ψ-Shaped UWB Antenna with Dual Band Notched Characteristics. *Wireless Personal Communications,* 89, 79–92.

[48] Rahmana MU, Khan WT and Imran M (2018). Penta-notched UWB antenna with sharp frequency edge selectivity using combination of SRR, CSRR and DGS. *International Journal of Electronics and Communications (AEÜ),* 93, 116–122.

[49] Zhu F et al (2013). Multiple Band-Notched UWB Antenna With Band-Rejected Elements Integrated in the Feed Line. *IEEE Transactions on Antennas and Propagation,* 61 (8), 3952–3960.

CURRICULUM VITAE

Paramita Maiti has completed her Bachelor in Engineering degree in Electronics and Communication Engineering from Thapar Institute of Engineering and Technology, Patiala, Punjab in 2016. In 2016, she joined Master in Engineering program in Electronics and Communication Engineering at Thapar Institute of Engineering and Technology, Patiala, Punjab. During ME-ECE, she worked on the topic "Design of Planar and Compact UWB microstrip antenna with band rejection features" for her thesis work. Recently, her paper entitled 'A split ring resonators based printed compact monopole UWB antenna with spiked elliptical radiator having five band rejection features' has been communicated to International Journal of Microwave and Wireless Technologies.

LIST OF PUBLICATIONS

1. Maiti P and Kaur J. (2018). A split ring resonators-based printed compact monopole UWB antenna with spiked elliptical radiator having five band rejection features, *International Journal of Microwave and Wireless Technologies (First Review).*

2. Maiti P and Kaur J. (2018). A Compact Stepped Monopole Triple Band-Notched UWB Antenna with a Composite Parasitic Element, *Microwave and Optical Technology Letters*. (Under Preparation)